Clinical Immunology 254 (2023) 109684

Contents lists available at ScienceDirect

Clinical Immunology

journal homepage: www.elsevier.com/locate/yclim

SARS-COV-2 specific t-cells in patients with thyroid disorders related to COVID-19 are enriched in the thyroid and acquire a tissue-resident memory phenotype

Ylenia Silvestri [a], Francesca Clemente [a], Giorgia Moschetti [a], Sara Maioli [b], Elena Carelli [a], Alejandro Espadas de Arias [c], Rosanna Torelli [c], Elena Longhi [c], Tullia De Feo [c], MariaCristina Crosti [a], Maria Lucia Sarnicola [a], Mario Salvi [d], Giovanna Mantovani [b,d], Maura Arosio [b,d], Mauro Bombaci [a], Elisa Pesce [a], Renata Grifantini [a], Sergio Abrignani [a,b], Jens Geginat [a,b,1,*], Ilaria Muller [b,d,1,*]

[a] Istituto Nazionale Genetica Molecolare Romeo ed Enrica Invernizzi, Milan, Italy
[b] Dipartimento di Scienze Cliniche e di Comunità, Università di Milano, Milan, Italy
[c] S.C. Trapianti Lombardia - NITp, Fondazione IRCCS Cà Granda Ospedale Maggiore Policlinico, Via Sforza 35 c/o INGM, 20122 Milano, Iraly
[d] Struttura Complessa Endocrinologia, Fondazione IRCCS Ca' Granda Ospedale Maggiore Policlinico, Milan, Italy

ARTICLE INFO

Keywords:
SARS-COV2
Tissue resident memory cells
Thyroid
Anti-viral T-cells

ABSTRACT

Background: SARS-CoV-2 infections have been associated with the onset of thyroid disorders like classic subacute thyroiditis (SAT) or atypical SAT upon severe COVID disease (COV-A-SAT). Little is known about thyroid anti-viral immune responses.
Objectives: To define the role of T-cells in COV-A-SAT.
Methods: T-cells from COV-A-SAT patients were analyzed by multi-dimensional flow cytometry, UMAP and DiffusionMap dimensionality reduction and FlowSOM clustering. T-cells from COVID-naïve healthy donors, patients with autoimmune thyroiditis (ATD) and with SAT following COVID vaccination were analyzed as controls. T-cells were analyzed four and eight months post-infection in peripheral blood and in thyroid specimen obtained by ultrasound-guided fine needle aspiration. SARS-COV2-specific T-cells were identified by cytokine production induced by SARS-COV2-derived peptides and with COVID peptide-loaded HLA multimers after HLA haplotyping.
Results: COV-A-SAT was associated with HLA-DRB1*13 and HLA-B*57. COV-A-SAT patients contained activated Th1- and cytotoxic CD4+ and CD8+ effector cells four months post-infection, which acquired a quiescent memory phenotype after eight months. Anti-SARS-CoV-2-specific T-cell responses were readily detectable in peripheral blood four months post-infection, but were reduced after eight months. CD4+ and CD8+ tissue-resident memory cells (TRM) were present in the thyroid, and circulating CXCR3+T-cells identified as their putative precursors. SARS-CoV-2-specific T-cells were enriched in the thyroid, and acquired a TRM phenotype eight months post-infection.
Conclusions: The association of COV-A-SAT with specific HLA haplotypes suggests a genetic predisposition and a key role for T-cells. COV-A-SAT is characterized by a prolonged systemic anti-viral effector T-cell response and the late generation of COVID-specific TRM in the thyroid target tissue.

1. Introduction

Since early 2020 the pandemic of Coronavirus disease 2019 (Covid-19), determined by the severe acute respiratory syndrome coronavirus 2 (SARS-CoV-2), has represented an unprecedented global health emergency [1]. Since the end of 2020, one of the main sanitary measures implemented to fight the Covid-19 pandemic has been the launch of the greatest and fastest mass vaccination in human history [2,3]. In Italy,

* Corresponding authors at: Dipartimento di Scienze Cliniche e di Comunità, Università di Milano, Milan, Italy.
[1] Equal contributions

https://doi.org/10.1016/j.clim.2023.109684
Received 28 March 2023; Received in revised form 7 June 2023; Accepted 21 June 2023
Available online 13 July 2023

where our Institution is located, 4 types of Covid-19 vaccines have been used, all encoding for the SARS-CoV-2 spike protein: two mRNA lipid nanoparticle vaccines (BNT162b2 Comirnaty®, Pfizer−BioNTech and mRNA-1273 SpikeVax®, Moderna) and two DNA (adeno)viral vector vaccines (Vaxzevria® Astrazeneca and Janssen® Johnson&Johnson) [2]. Both SARS-CoV-2 infection and Covid-19 vaccines induce specific CD4+ and CD8 + T-cell responses that can be detected in the circulation even after several months [4–6]. In the lung, virus-specific T-cells can become tissue-resident cells, which do not recirculate but can provide immediate protection [7,8]. Notably, anti-SARS-CoV-2 immune responses have been associated with the onset of thyroid disorders [9,10]. In particular, after SARS-CoV-2 infection several cases of subacute thyroiditis (SAT) and autoimmune thyroid disorders (ATD) have been described [11–14]. We have described the onset of atypical thyroiditis in hospitalized patients for severe Covid-19 disease, as the result of painless thyroiditis associated to non-thyroidal illness syndrome [15,16]. Similarly, cases of SAT [17–20] or ATD such as Graves disease and Graves' orbitopathy [21–26] have been described following Covid-19 vaccination. However anti-SARS-CoV-2 immune responses in the thyroid have not been investigated in detail yet [9,10]. In the present study we therefore characterized the immunological response to SARS-CoV-2 in patients with non-autoimmune atypical thyroiditis developed during severe Covid-19 disease (COV-A-SAT). We analyzed anti-viral CD4+ and CD8+ T-cell subsets by immunophenotyping and tested their SARS-CoV-2 specificity both in peripheral blood and thyroid-infiltrating T-lymphocytes. We observed a systemic anti-COVID effector T-cell response 4 months post-infection that largely vanished after 8 months, and the concomitant late generation of COVID-specific TRM in the thyroid.

2. Materials and methods

2.1. Study population

The study included 13 patients having developed atypical thyroiditis during severe COVID-19 disease (COV-A-SAT), 6 patients developing classic SAT following COVID-19 vaccination (VAX-SAT) and 6 patients with ATD (3 spontaneous and 3 following COVID-19 vaccination) followed at the IRCCS Fondazione Ca' Granda Ospedale Maggiore Policlinico, Milan, Italy (Table 1). Four of the COV-A-SAT patients had concomitant ATD and were thus excluded from the analysis, unless indicated (Fig. 6C, Fig. 7 and Table 2). Fifteen healthy donors (HD) previously unexposed to SARS-CoV-2 were also included in the study as controls. To this purpose the presence of IgG anti-spike protein (anti-S IgG) in serum was determined by ELISA to verify that HD had negative anti-S IgG [5].

The COV-A-SAT group included patients developing non-autoimmune transient atypical thyroiditis during hospitalization for severe Covid-19 disease, defined as painless transient thyrotoxicosis (low/suppressed TSH and/or elevated FT4), or presence of hypoechoic areas of thyroiditis at thyroid ultrasound [15,16]. COV-A-SAT patients were tested positive for COVID-19 by real-time reverse transcriptase polymerase chain reaction conducted on nasal and pharyngeal swab specimens for a period of 37±15 days (range 17–69 days).

All patients in the VAX-SAT group had non-autoimmune classic SAT, defined as classic painful transient thyrotoxicosis in presence of hypoechoic areas of thyroiditis at thyroid ultrasound [27]. The ATD group included 4 patients with Graves' disease (autoimmune hyperthyroidism with positive autoantibodies to thyrotropin receptor) complicated with Graves' orbitopathy (thyroid-related orbital tissue inflammation [28]), one patient with Graves' disease without ocular complications and one patient with euthyroid autoimmune thyroiditis in multinodular goitre. The VAX patients developed thyroid disorders 15 ± 18 (mean ± SD) days after receiving the last dose of Covid-19 vaccine. At timepoint I (4 months), all COV-A-SAT and one ATD patients were euthyroid in absence of treatment, while the majority of VAX-SAT and ATD patients were thyrotoxic (Table 1). Importantly, none of the COV-A-SAT patients had been vaccinated for Covid-19 at both time-points, since sampled before the launch of the mass vaccination campaign. Similarly, none of the ATD patients had a known previous infection with SARS-CoV-2, except for one case who had symptomatic Covid-19 disease two months before receiving Covid-19 vaccination.

This study was approved by the ethical committee of Milano Area 2 (permissions 0004946 69_2020bis 7/2/2020 ID 1333 and 583_2021 5/5/2021 ID 1582) and informed consent was obtained from all subjects.

Table 1
Patient characteristics.

	HD	ATD	VAX-SAT	COV-A-SAT
	(*n* = 15)	(*n* = 6)	(*n* = 6)	(*n* = 13)
Female sex *N (%)*	6 (40)	5 (83)	3 (50)	6 (46)
Age years *mean (SD)*	44 (14)	54 (11)	55 (14)	60 (9)
Timepoint I days *mean (SD)* [1]	NA	115 (83) [2]	88 (30)	120 (39)
Timepoint II days *mean (SD)* [1]	NA	NA	NA	243 (8)
Previous thyroid disorders *N (%)*	NA	2 (67) [2]	1 (16)	0 (0)
Thyroid family history *N (%)*	NA	5 (83)	4 (67)	1 (8)
TSH mIU/l *median (IQR)*	1.43 (0.83)	0.02 (0.38)	0.06 (0.46)	1.65 (0.90)
FT4 ng/l *mean (SD)*	NA	23.3 (26.9)	14.2 (6.8)	11.1 (1.8)
FT3 ng/l *mean (SD)*	NA	7.3 (7.5)	3.4 (1.1)	3.1 (0.4)
TRAb POS *N (%)*	NA	5 (83)	0 (0)	0 (0)
TPOAb POS *N (%)*	0 (100)	5 (83)	0 (0)	2 (15)
TgAb POS *N (%)*	0 (100)	4 (67)	0 (0)	2 (15)
Steroids *N (%)*	NA	1 (17)	3 (50)	0 (0)
Anti-thyroid drugs *N (%)*	NA	4 (67)	0 (0)	0 (0)
Levothyroxine *N (%)*	NA	0 (0)	0 (0)	0 (0)

General and clinical characteristics of patients developing atypical thyroiditis during severe Covid-19 (COV-A-SAT), subacute thyroiditis after Covid-19 vaccination (VAX-SAT), autoimmune thyroid disorders (ATD) and healthy donors (HD).
Abbreviations: FT3 = free-tri-iodothyronine, FT4 = free-thyroxine, IQR = interquartile range, NA = Not applicable, SD = standard deviation, TgAb = autoantibodies to thyroglobulin, TPOAb = autoantibodies to thyroid peroxidase, TRAb = autoantibodies to the TSH receptor, TSH = thyroid stimulating hormone.
1 = Days between blood/thyroid assessment and date of SARS-CoV-2 positive test (Covid-19 group) or last dose of Covid-19 vaccine (VAX-SAT and ATD groups).
2 = Figures apply only to the three patients developing ATD following Covid-19 vaccination.

2.2. Human samples

Paired blood withdrawal and ultrasound-guided fine needle aspiration (US-FNA) of thyroid gland were obtained from patients, while HD underwent blood withdrawal only. Blood sampling and thyroid US-FNA were performed four months post-infection or vaccination in all patients. Five COV-A-SAT patients were also analyzed for paired blood and thyroid sampling 8 months after infection. Notably, due to the limited and variable number of cells obtained from human samples, not all assays could be performed with all patients.

2.3. Thyroid analysis

The serum concentrations of thyroid stimulating hormone (TSH), free-thyroxine (FT4) and tri-iodothyronine (FT3) were measured by electrochemiluminescence immunoassay (Cobas® e801, Roche Diagnostics). Reference intervals were 0.28–4.30 mIU/l for TSH, 8–17 ng/l for FT4 and 2–5 ng/l for FT3. Autoantibodies to thyroid peroxidase (TPOAb) and thyroglobulin (TgAb) were measured by enzyme-linked

Table 2
Human Leucocytes Antigen (HLA) typing.

	Allele I	Allele II
FNA1	A*01:01	A*01:01
	B*35:02	B*57:01
	C*04:01	C*06:02
	DRB1*07:01	DRB1*11:04
FNA2	A*02:11	A*30:01
	B*35:01	B*44:03
	C*04:01	C*04:01
	DRB1*04:07	DRB1*15:03
FNA3	A*03:01	A*24:02
	B*35:01	B*44:02
	C*04:01	C*05:01
	DRB1*01:01	DRB1*13:01
FNA4	A*24:02	A*26:01
	B*35:08	B*44:02
	C*04:01	C*05:01
	DRB1*13:01	DRB1*13:02
FNA5*	A*02:01	A*11:01
	B*15:17	B*57:01
	C*06:02	C*07:01
	DRB1*07:01	DRB1*13:02
FNA6	A*01:01	A*02:05
	B*35:01	B*58:01
	C*06:02	C*07:18
	DRB1*08:04	DRB1*11:04
FNA7	A*03:01	A*11:01
	B*07:02	B*08:01
	C*07:02	C*07:18
	DRB1*03:01	DRB1*14:01
FNA8	A*02:02	A*23:01
	B*41:01	B*52:01
	C*12:02	C*17:01
	DRB1*13:03	DRB1*15:02
FNA9	A*03:01	A*24:02
	B*18:01	B*51:01
	C*07:02	C*12:03
	DRB1*07:01	DRB1*13:02
FNA10*	A*01:01	A*24:17
	B*15:02	B*57:01
	C*06:02	C*08:01
	DRB1*07:01	DRB1*12:02
FNA11	A*24:02	A*68:02
	B*35:03	B*53:01
	C*04:01	C*12:03
	DRB1*01:02	DRB1*11:01
FNA12	A*01:01	A*01:01
	DRB1*01:01	DRB1*11:04
FNA13	A*02:01	A*02:01
	DRB1*13:01	DRB1*16:01

Human Leucocytes Antigen (HLA) typing of locus A, B, C and DRB1 of COVID-19 patients ($n = 13$).
Patients expressing HLA-A*24:02, HLA-A*01:01, HLA-A*02:01 or HLA-DRB1*07:01 eligible for dextramers staining are highlighted in grey. FNA1, FNA2, FNA7 and FNA13 also had thyroid autoimmunity.
* Although FNA5 and FNA10 patients had eligible haplotypes, we had insufficient thyroid material to perform dextramers analysis.

immunosorbent assay (ThermoFisher) and autoantibodies to TSH receptor (TRAb) by Immulite 2000/2000 XPi TSI (Siemens). Normal reference ranges were < 35 KIU/L (TPOAb), < 60 KIU/L (TgAb) and < 0.55 KIU/L (TRAb). Serum was tested for TgAb with ELISA kit (EIA-3708, Pantec), TPOAb (EIA-3561, Pantec) and TSH (EHTSH, Invitrogen). Normal reference ranges were < 100 IU/ml (TgAb), < 50 IU/ml (TPOAb) and between 0.2 and 4.3 mIU/l (TSH). Excluding the ATD group, all patients that were positive for TPOAb or TgAb, which is quite common in the general population (12%) [29], were excluded from the analysis unless indicated (Fig. 6C, 7 and Table 2).

2.4. Cell isolation

Human peripheral blood mononuclear cells (PBMCs) were isolated by using Ficoll-Hypaque (Sigma-Aldrich) gradient. Lymphocytes from thyroid US-FNA were processed or frozen immediately after collection, without isolation procedures.

2.5. Intra-thyroid detection of SARS-CoV-2 mRNA

The presence of intra-thyroid SARS-CoV-2 RNA on thyroid US-FNA samples was tested by real-time reverse transcriptase polymerase chain reaction with GeneFinder™ 2019-nCoV RealAmp Kit (IFMR-29) and AllplexTM 2019-nCoV Assay (Seegene).

2.6. Ex vivo flow cytometric analysis of T-lymphocytes

Flow cytometry was performed according to the published guidelines [30]. PBMCs were stained at the cell surface with the following antibodies: CD4 (OKT4, Invitrogen or SK3, BD Biosciences), CD103 (Ber-ACT8, BD Biosciences), CD25 (M-A251 or 2A3 BD Biosciences), CD38 (HIT2, BD Biosciences), CD27 (M-T271 or L128, BD Biosciences), CD127 (AO19D5, Biolegend or HIL-TI7R-M21, BD Biosciences), CD45 (2D1, Biolegend), CD8 (SK1 or RPA-T8, BD Biosciences), CD69 (FN50, BD Biosciences), CXCR3 (1C6/CXCR3, BD Biosciences), CCR7 (150,503, BD Biosciences), LIVE/DEAD™ (Thermo Fisher Scientific), CD45RA (HI100, BD Biosciences), CD56 (B159, BD Biosciences) and CD3 (UCHT1, BD Biosciences or Biolegend). For the analysis of intracellular markers, cells were fixed and permeabilized and stained intracellularly for Foxp3 (259D, Biolegend), Granzyme K (GM6C3, Santa Cruz), CD40L (24–31, Biolegend), Granzyme B (GB11, BD Biosciences), Eomes (WD1928, Invitrogen), IFN-γ (B27, BD Biosciences), Ki67 (B56, BD Biosciences), IL-2 (5344.111, BD Biosciences) and TNF-α (Mab11, BD Biosciences). Samples were acquired at FACS Symphony cell analyser (BD Biosciences) and data were analyzed using FlowJo Software.

2.7. Bioinformatic analysis

Flow cytometry data were imported into FlowJo software (version 10.8.0) to compensate fluorescence spreading; dead cells, debris, B cells and monocytes were excluded from the analysis. To compare the blood of patients versus those of HD a random down-sample of 5000 events for CD3+ T-cells compartment was performed. In order to compare blood and thyroid of the same patient (paired) a random down-sample of 1620 events was performed separately for CD4+ and CD8+ T-cells. Finally, CD4+ and CD8+ down sampled data where merged and exported as FCS file for further analysis in R software (version 4.0.2).

Sample batches were read using read.flowSet (2.6.0) from the flowCore R package. We applied the Logicle transformation that allows the use of multiple samples to estimate transformation parameters. To reduce batch effect due to technical and not to biological variation we normalized the signal of each marker with the function gaussNorm from the flowStat package (4.6.0). After the batch-specific pre-processing, samples were concatenated into a SingleCellExperiment object in R using the function prepData from the CATALYST R package [31]. Dimensionality reduction by UMAP was subsequently applied to visualize relative proximities of cells within reduced dimensions. We performed high-resolution, unsupervised clustering and meta-clustering using FlowSOM (2.2.0) and ConsensusClusterPlus (1.58.0) packages following the workflow in Nowicka et al. [31]. The T-cell compartment in the comparison of blood and thyroids belonging to the same patient (paired analysis) was clustered based on the expression of 11 markers: CD4, CD8, CD127, CD27, CD38, CD25, CXCR3, CD103, CD69, Ki67 and CD56. Whereas, in the analysis of blood of patients and HD, T-cells were clustered based on the following markers: CD4, CD8, CD45RA, CCR7, CD27, CCR5, CXCR3, CD25, FOXP3, EOMES, GRANZYME K, GRANZYME B, PD1, CD69 and Ki67. In addition, CD127 was included in the comparison of COV-A-SAT patients at 4 and 8 month post-infection. Manually annotated clusters were subsequently visualized on the UMAP. Functional pseudo-time analysis to infer the differentiation trajectory of cells was carried out by Diffusion Maps [31] using the function

run Diffusion Map on the SingleCellExperiment object using default parameters. We performed, also, a dimensionality reduction plot on centered log-ratios (CLR) of sample/cluster proportions across cluster/samples, in order to understand similarities between samples/clusters based on their composition.

2.8. Antigenic stimulation

Stimulation with SARS-CoV-2 peptides was performed for 5 h with 1×10^6 PBMCs in RPMI complete medium (2 mM glutamine, 1 mM sodium pyruvate, 1% non-essential amino acids, 1% penicillin/streptomycin) supplemented with 5% of autologous plasma and 1μg/ml of PepTivator SARS-CoV-2 Spike protein, Membrane protein or Nucleocapsid protein (Miltenyi Biotec) for 5h at 37°C in a 5% CO_2 humidified atmosphere. Cytokine secretion was blocked with 0,6 μl/ml Monensin (Golgi Stop Protein Transport Inhibitor, 554,724, BD Biosciences) after 90 min of incubation. To calculate the T-cells response data were normalized by subtraction of unstimulated value.

2.9. Human Leukocyte Antigen (HLA) Typing and HLA dextramer stainings

HLA typing of locus A and DRB1 was performed in all COV-A-SAT patients, i.e. including in this case also the four patients with concomitant ATD, by reverse dot blotting (RDB) bead array with LabType SSO XR kits (One Lambda, Inc.) (Table 2). Seven patients expressing HLA-A*24:02, and/or HLA-A*01:01, or HLA-A*02:01 and/or HLA-DRB1*07:01 were analyzed with commercially available, relevant dextramers for the presence of COVID-specific T-cells (Table 3). Notably, the HLA-A*02:01+ FNA13 and the HLA-DRB1*07:01 FNA1 had concomitant ATD, but were nevertheless analyzed with dextramers (Fig. 7). COVID-19-specific T-cells in thyroid fine needle aspiration or peripheral blood were detected by staining with CD4 (RPA/T4, BD Biosciences) or CD8 (SK1, BD Biosciences), CD69 (FN50, BD Biosciences) and CD103 (Ber-ACT8, BD Biosciences), along with MHC II (FE10157, FE10172, Immudex) or MHC I dextramer (WF05952, WF06097, WA05846, WB5824, WB05838, Immudex). The cells were acquired at Aria III cell sorter (BD Biosciences) and data were analyzed using FlowJo Software.

2.10. Amino acid sequence homology between SARS-CoV-2 and thyroid auto-antigens

To investigate potential amino acid sequence similarities between the spike protein of SARS-CoV-2 and other proteins, namely TPO, TSHR, and TG, we utilized the BLAST (Basic Local Alignment Search Tool) sequence matching program provided by the NIH/US National Library of Medicine. Additionally, we employed Clustal Omega to determine the presence of similar proteins among amino acid groups. In the Clustal Omega results, the conservation between strongly similar property groups is denoted by ":" while conservation between weakly similar property groups is denoted by ".".

Table 3
Covid-19 T-cells Epitopes.

HLA Allele	MHC	Antigen	Peptide
A*2402	Class I	Spike (S2)	QYIKWPWYI
A*2402	Class I	Spike (RBM)	NYNYLYRLF
A*0101	Class I	Spike (S2)	LTDEMIAQY
A*0201	Class I	Spike (NTD)	YLQPRTFLL
A*0201	Class I	Spike (RBD)	KLPDDFTGCV
DRB1*0701	Class II	Spike (S2)	QLIRAAEIRASANLAAT
DRB1*0701	Class II	Envelope	FYVYSRVKNLNSSRV

Covid-19 T-cells Epitopes used to analyze the presence of COVID-specific T-cells in thyroid fine needle aspiration and peripheral blood of seven COV-A-SAT patients.

2.11. MHC class I epitope prediction

We utilized the NetMHCpan-4.1 server [32] to predict peptide binding to MHC class I molecules. The protein sequences of thyroid peroxidase (TPO, UniProt: P07202, 933aa), thyrotropin receptor (TSHR, UniProt: P16473, 764aa), and thyroglobulin (TG, UniProt: P01266, 2768aa) were inputted in FASTA format. The following parameters were applied: peptide length of 9–11 amino acids, threshold for strong binder (SB) set at 0.5% rank, and threshold for weak binder (WB) set at 2% rank. Short peptides of 9–11 amino acids were generated, and only those classified as strong binders (SB) were evaluated to identify candidate epitopes with high affinity for the HLA alleles A*01:01, A*02:01, A*24:02, and the COV-A-SAT-associated risk allele HLA-B*57:01.

2.12. Statistics

All data comparisons were performed using GraphPad Prism 8 software. Statistical significance for multiple comparison was calculated using Mann Whitney test, one-way ANOVA with Kruskal-Wallis post-test or two-way ANOVA with Turkey's post-test. Statistical significance for longitudinal analysis was calculated using paired student's t-test. $p < 0.05$(*), $p < 0.01$(**), $p < 0.001$(***) and $p < 0.0001$(****) were regarded as statistically significant. Error bars reflect ± SEM.

The chi-squared test was applied to test for the HLA association between two categorical variables. Fisher's exact test was performed in case of having a frequency of <5 in one or more of the cells. Statistical significance was determined at $p < 0.05$. Statistical analyses were performed using SAS 9.4.

3. Results

3.1. Th1 and cytotoxic T-cell clusters are increased in patients with COVID-induced atypical thyroiditis (COV-A-SAT)

We first studied if, four months post-infection, the composition of the T-cell compartment in peripheral blood of COV-A-SAT patients showed major alterations compared to COVID-naïve healthy donors (HD). Patients that developed subacute thyroiditis following vaccination (VAX-SAT) and those with autoimmune thyroid disorders (ATD, for details see Materials Methods) were analyzed as additional controls. Five patients per group were analyzed by multiparametric flow cytometry and unsupervised clustering performed. Seventeen different clusters were identified, eight CD4+, eight CD8+ and one CD4-CD8- T-cell cluster (Fig. S1A). There were strong differences in the frequencies of these T-cell clusters in COV-A-SAT patients as compared to HDs (Fig. 1A). Importantly, several clusters that were increased in COV-A-SAT patients (i.e., CD4: Clusters 2, 4, 6–8; CD8: Clusters 10, 11, 15 and 17) expressed markers that are characteristic for Th1 (i.e., CXCR3) and/or cytotoxic T-cells (i.e., Eomes and Granzymes (Gzm, K or B)), i.e. T-cell subsets that mediate anti-viral immune responses. However, many clusters were also increased in VAX-SAT and in particular in ATD patients (Fig. 1A, B and S1B). Consistently, the first two principal components computed on CLR plot unveiled that the T-cell cluster composition of COV-A-SAT patients were quite similar to that of ATD patients and more distinct from VAX-SAT patients and HDs (Fig. S1C). We next analyzed the 17 T-cell clusters by Diffusion Map that models possible differentiation pathways in pseudo-time. Both CD4+ and CD8+ T-cells showed a predicted differentiation pathway from naïve T-cells (Clusters 1, 9), i.e. uncommitted precursor cells, to cytotoxic T-cells expressing GzmB (Clusters 7 (CD4) and 13–15 (CD8), Fig. 1C and S1D), which are indeed considered to be terminally differentiated effector cells. Clusters at an intermediate stage of differentiation (CD4: Clusters 2–6, CD8: Clusters 11, 12 and 16) corresponded to memory-like cells (Fig. S1D). Diffusion Map analysis predicted a progressive differentiation from clusters containing CCR7+ central memory T-cells (T_{CM}, Clusters 2–5 (CD4) and 11 (CD8)) to CCR7- effector memory clusters (TEM, Clusters 6, 8 (CD4) and 12, 16 (CD8)), as

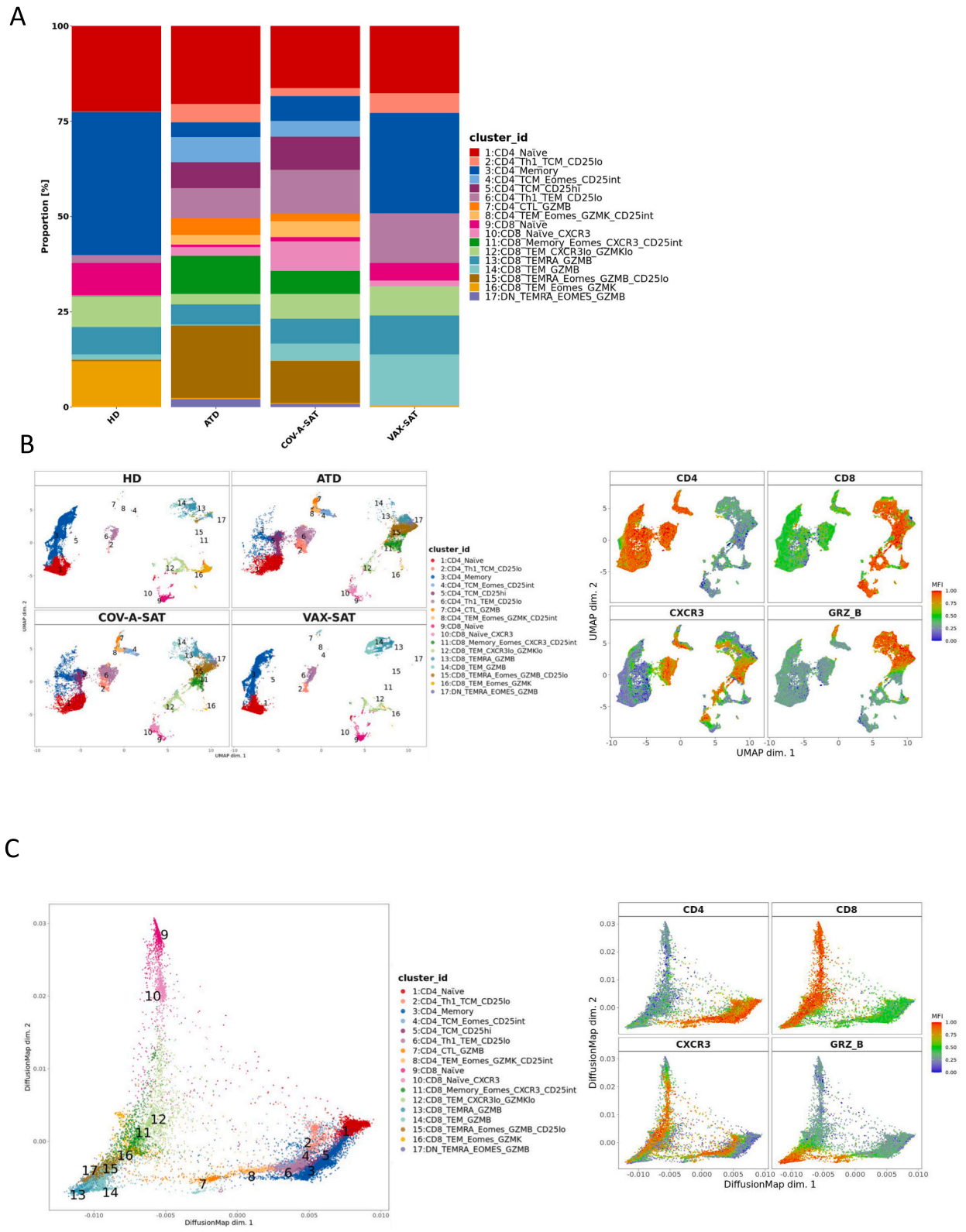

Fig. 1. COVID-induced subacute thyroiditis (COV-A-SAT) is associated with Th1 and cytotoxic T-cell clusters.

A. Bar-plots showing selective cluster distributions in the blood of healthy donors (HD), autoimmune thyroiditis patients (ATD) and patients with subacute thyroiditis following vaccination (VAX-SAT) or COVID infection (COV-A-SAT). The 17 subsets corresponding to the different colors are listed in the panel.

B. Left: UMAP maps of the four patient cohorts (all $n = 5$) colored according to the 17 identified T-cell clusters. Numbers in the UMAP maps indicate the 17 clusters. Right: UMAP of CD4, CD8, CXCR3 and GZM_B expression.

C. Left: Diffusion Map modelling differentiation pathways from naïve T-cells to GZMB+ CTL. The 17 identified clusters are indicated by numbers and cluster-specific colors.

Right: DiffusionMap of CD4, CD8, CXCR3 and GZM_B expression.

B/C: (Right panels) Red indicates high, green intermediate and blue low expression levels.

expected [33]. Moreover, CCR5 and GzmK were restricted to TEM clusters, while CXCR3 was also expressed on less differentiated TCM-like clusters [34].

In summary, unbiased bioinformatical analysis identified in COV-A-SAT patients several different CD4+ and CD8+ T-cell memory- and effector-like clusters, which contained cells that are involved in anti-viral immune responses.

3.2. Cytotoxic and effector T-cells are still increased in the blood of patients with COVID-induced atypical thyroiditis (COV-A-SAT) four months post-infection

To corroborate the above finding, we performed conventional manual gating of canonical T-cell subsets. Total CD3+, CD4+ and CD8+ T-cells did not show significant differences between the 4 cohorts (Fig. S2A). Also the major subsets associated with progressive T-cell differentiation, i.e. naïve, central memory and effector memory subsets (CD45RA-TEM and CD45RA + TEMRA) did not show significant alterations in COV-A-SAT patients (Fig. S2B). Conversely, we detected significant increases of CD4+CTL (GzmB+) in all three patients' cohorts as compared to HDs (Fig. 2A). Also Th1-cells (CXCR3+[34]) were in mean more frequent in the patients, but these increases did not reached statistical significance (Fig. 2A). Conversely, the frequencies of regulatory T-cell (Treg) subsets, i.e. FOXP3+Tregs and Tr1-like cells [35], were not significantly different in the four cohorts (Fig. S2C).

We next assessed the expression of surface markers that are modulated upon T-cell activation. Thus, we monitored expression of CD69 and CD38, which are induced upon activation, and of IL-7R and CD27, which are in contrast down-regulated upon activation and/or effector cell generation [36–38]. Total CD4+T-cells and CD8+ T-cells did not express increased levels of CD69 or CD38, but in COV-A-SAT patients they expressed overall lower levels of CD27 and IL-7R (Fig. S2D). In particular, CD4+CTL in all patients cohorts had down-regulated IL-7R and CD27 expression, but the acquisition of an IL-7R_{low}CD27- effector phenotype was most evident in COV-A-SAT patients (Fig. 2B). The majority of Th1-cells displayed in contrast as expected an IL-7R_{high}CD27+ memory phenotype, in particular in COV-A-SAT and VAX-SAT patients, but they contained nevertheless also some effector-like cells (Fig. 2B).

Among CD8+T-cells we also detected a significant increase of canonical cytotoxic GzmB+ T-cells in all three patient cohorts (Fig. 2C), and this increase was again most prominent in COV-A-SAT patients. Moreover, cytotoxic CD8+GzmB+ cells in COV-A-SAT patients had again a significantly more pronounced IL-7R_{low}CD27- effector phenotype (Fig. 2D). Also the less differentiated cytotoxic GzmK+CD8+ cells [39] (Fig. 1C) had a more effector-like phenotype in COV-A-SAT patients, and contained in particular significant lower frequencies of cells with an IL-7R_{high}CD27+ memory phenotype (Fig. 2D).

We then evaluated the proliferation rates of T-cells according to intracellular Ki67 expression, which marks cells that have divided in the last few days in vivo [40]. Although the virus in the serum of all COV-A-SAT patients was undetectable since several weeks (81±39d, range 24-179d), there was still an increase of proliferating CD4+ and CD8+T-cells in COV-A-SAT patients (2.897±0.567% (CD4) and 2.991±0.816% (CD8)) as compared to COVID-naïve HD (1.433±0.262% (CD4) and 1.461±0.326% (CD8), Fig. 2E). Notably, we did not observe an inverse association between this increased T-cell proliferation and the time that patients became seronegative for the virus (data not shown). Among CD4+T-cells, the proliferation of cells with a CD45RA+CCR7+ phenotype, which is characteristic not only for naïve but also for memory stem cells [41], was significantly increased (Fig. S2E). Moreover, Th1-cells (Fig. 2F) and regulatory T-cells (Fig. S2F) showed increased proliferation rates selectively in COV-A-SAT patients. Among CD8+T-cell subsets, GzmK+ cells showed a significantly higher proliferation exclusively in COV-A-SAT patients (Fig. 2F).

In summary, COV-A-SAT patients still showed moderately increased in vivo T-cell proliferation in peripheral blood four months post-infection, and in particular CD4+ and CD8+ cytotoxic effector T-cells were significantly increased.

3.3. The increase of activated effector T-cells in the blood of COV-A-SAT patients is transient

Five COV-A-SAT patients could be analyzed at two different time points, i.e., four and eight months after SARS-CoV-2 infection (Table 1). Notably, the virus was already undetectable at the earlier time point, not only in the serum, but also in the thyroid (data not shown). Thus, the analyzed two time points represent an early and a late time point of immunological memory generation.

Strikingly, unsupervised cluster analysis of the two time points (Fig. S3A—B) unveiled that in the CD4 compartment there was a clear shift from Th1 effector cells (Cluster 4) to Th1 central memory cells (Cluster 3, Fig. 3A). We also detected a marked decrease of several CD4-CD8- T-cell clusters (DN, Clusters 15–17), whereas the dynamics among different cytotoxic CD8+T-cell clusters (Clusters 8–14) was more subtle and complex (Fig. 3A). Conventional manual gating unveiled that both CD4+ and CD8+ central memory subsets increased significantly at the late time point, while CD4+ effector memory subsets were instead significantly reduced (Fig. S3C). Also regulatory T-cell subsets decreased slightly over time (Fig. S3D). There were in contrast no consistent changes in the frequencies of CD4 CTL and Th1-cells (Fig. 3B). In the CD8 compartment we observed, in contrast, a significant and selective decrease of cytotoxic T-cells that expressed GzmK (Fig. 3B). Both CD4+ and CD8 + T-cells showed moreover a reduction of proliferating Ki67+ cells at the later time point, in particular in the patients with higher proliferation rates at the earlier time point (Fig. 3C). Similar tendencies of reduced proliferation at the later time point were observed for Th1, CD4+CTL and cytotoxic CD8+T-cell subsets, which reached statistical significance for CD8+GzmK+T-cells (Fig. 3D). Also regulatory T-cell subsets showed reduced proliferation at the late time point in most patients (Fig. S3E).

Finally, we also monitored the dynamics of activation marker expression. CD4 + T-cells expressed significantly lower levels of CD69 after 8 months, and both CD4+ and CD8+ T-cells up-regulated IL-7R and CD27 expression (Fig. S3F). IL-7R was significantly up-regulated on CD+CTL and in particular on Th1-cells, consistent with an effector-to-memory transition, as suggested by Fig. 3A. IL-7R re-expression was less prominent on cytotoxic CD8 +T-cell subsets, but CD27 was significantly up-regulated on CD8 + GzmK+ T-cells (Fig. 3D). Notably, the latter also showed the most marked increases of CCR7 (Fig. 3D) and of CXCR3 (Fig. S3G).

In conclusion, the increases in T-cell proliferation and anti-viral effector cells in COV-A-SAT patients observed in the early memory phase was transient and returned to normal levels 8 months post infection.

3.4. Early robust COVID-specific T-cell responses in the blood of COV-A-SAT patients are not sustained

We next analyzed the specificity of CD4+ and CD8+ T-cells from peripheral blood in COV-A-SAT patients for COVID-19-derived antigens. T-cells were stimulated with SARS-CoV-2-derived peptide pools, and COVID-reactive T-cells identified according to the concomitant up-regulation of activation markers and cytokine production. COV-A-SAT patients, but not the COVID-19 inexperienced HDs, showed a variable, but clearly detectable IFN-γ response of CD4+CD40L+ helper T-cells with Spike (S), Membrane (M) and Nucleocapsid (N) protein-derived peptide pools 4 months post-infection (Fig. 4A). In addition, there was also a significant production of IL-2 by S-specific T helper cells, while TNF was hardly detectable (Fig. S4A). Notably, COVID-specific Th1-cells in the blood were overall strongly decreased after eight months. This was in particular true for patients that showed a strong response at the early time point (Fig. 4A). Notably, total activated (i.e., CD69+) CD4+T-

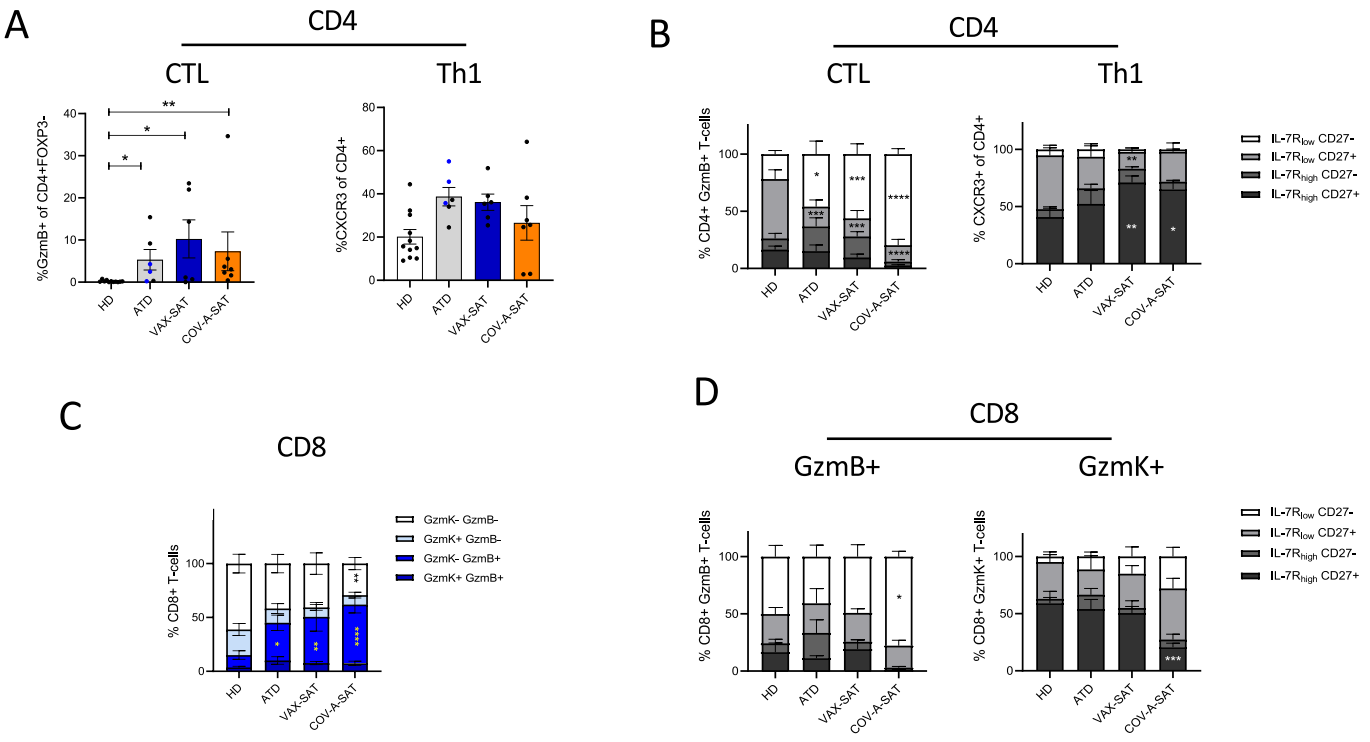

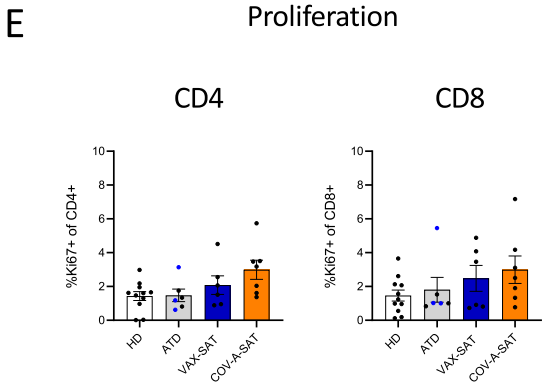

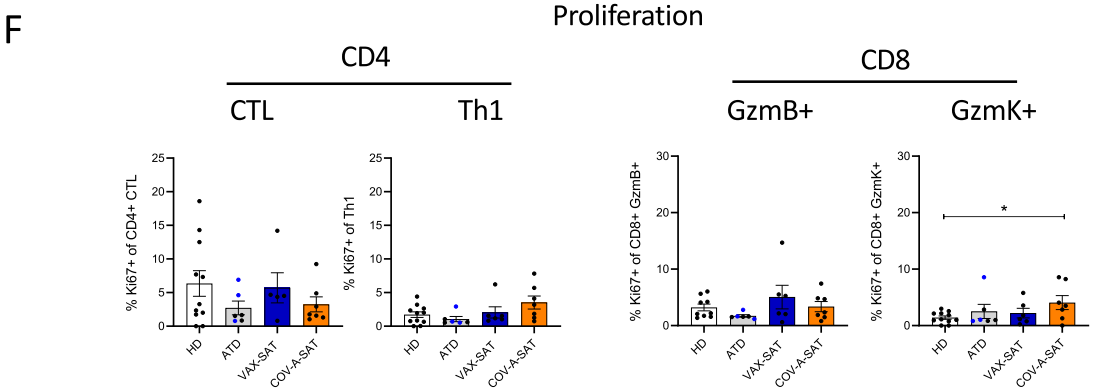

(caption on next page)

Fig. 2. Cytotoxic CD4+ and CD8+ effector cells are increased in COV-A-SAT.
COV-A-SAT patients (without ATD, $n = 7$) were compared to COVID-naïve HDs ($n = 11$), ATD ($n = 6$) and VAX-SAT ($n = 6$) patients.
A. Percentages of CTL (CD4+Foxp3-GzmB+) and Th1-cells (CD4+Foxp3-GzmK-GzmB-CXCR3+) among CD4+T-cells. Data show individual values and mean (bar heights) ± SEM.
B. Stacked histogram bars show expression of IL-7R and CD27 in CD4+ CTL and Th1-cells.
C. Expression of GzmB and GzmK in CD8+ T-cells in the same cohorts.
D. Stacked histogram bars show expression of IL-7R and CD27 in CD8+ GzmB+ and GzmK+ cells.
E. Proliferation of total CD4+ and CD8+ T-cells assessed by intracellular Ki67 staining ex vivo.
F. Proliferation of CD4+ CTL, Th1-cells, CD8+GzmB+ and GzmK+ T-cells.
A, *E*-F: Statistical analysis by one-way ANOVA; $p < 0.05$(*) and $p < 0.01$(**) were regarded as statistically significant; if not indicated, p value is not significant ($p > 0.05$).
B-D: Statistical analysis by two-way ANOVA; $p < 0.05$(*), $p < 0.01$(**), $p < 0.001$(***) and $p < 0.0001$(****) were regarded as statistically significant; if not indicated, p value is not significant ($p > 0.05$).

cells producing IFN-γ with COVID-derived peptides (Fig. S4B) were indeed predominantly Gzm-negative Th1-cells, but we detected also some GzmB+CTL specific for S, M and N four months post-infection that disappeared at the later time point (Fig. 4B).

In the CD8 compartment, the SARS-CoV-2 specific responses were overall rather low when total peripheral blood CD8+T-cells were analyzed (Fig. 4C). However, when GzmB+CD8+T-cells were analyzed separately, a more robust increase of IFN-γ production was evident in several patients after 4 months, but was again hardly detectable after 8 months (Fig. 4C). Also GzmK+CD8+ T-cells produced IFN-γ in some patients with S and N-derived peptides at the early time point (Fig. S4C), but not at the later time point. Finally, CD8+GzmB+T-cells were able to produce IL-2 and in particular TNF-α with Spike-derived peptides in some patients, but again only at the early time point (Fig. S4C).

In summary, COVID-specific Th1-cells as well as CD4+ and CD8+CTL were clearly detectable in the majority of COV-A-SAT patients in the blood four months post-infection, but they were hardly detectable after 8 months.

3.5. Unbiased analysis of T-cell phenotypes unveiled a differential distribution of T-cell clusters in the thyroid gland and the blood

To analyze immune responses also in the target tissue, we then compared T-cells from blood and thyroid samples obtained with US-FNA (see Material Methods). Since rather little is known on T-cells that infiltrate the thyroid gland, we first analyzed the T-cell compartments by unbiased multi-dimensional flow cytometry ex vivo. We selected one representative COV-A-SAT, one VAX-SAT and one ATD patient with a sufficiently high cellularity to perform unsupervised clustering [31]. In this analysis we identified 15 distinguishable major clusters (Fig. 5A), seven clusters were CD4+ and eight were CD8+ (Fig. 5B, Fig. S5A, B), and most clusters were enriched either in the blood or in the thyroid (Fig. 5A, C). Among CD4+ T-cells in the thyroid there was a strong enrichment of IL-7R+Th-cells (Cluster 1) and of CXCR3+Th1 cells (Cluster 3), which was related to CD56 expression on the corresponding Th and Th1 clusters in peripheral blood (Clusters 4 and 5; Fig. S5A). In addition, the CD25+Treg-containing clusters 6 and 7 were slightly reduced in the thyroid. Among CD8+T-cells, we observed mainly an enrichment of CD27- and IL-7Rlow effector-like cells (cluster 8 and 15, respectively) in the thyroid. In contrast, CD8+CXCR3+ clusters (12,13) were enriched in the blood. Intriguingly, a small cluster of highly activated and proliferating CD8+T-cells (Cluster 10) was identified in the blood, but was largely absent from the thyroid. Finally, cluster 14, which was composed of CD8+CD103+ cells, and contained also cells with a canonical CD103+CD69+ tissue-resident (TRM) phenotype, was enriched in the thyroid. The positioning of this cluster in the UMAP analysis suggested that TRM were distinct from all other CD8+ T-cells (Fig. S5B). Consistently, Diffusion Map analysis unveiled a clear differentiation pattern of TRM-cells, in particular of CD8+TRM, in the thyroid (Fig. 5C and Fig. S5C). Interestingly, among non-TRM-cells, clusters expressing CXCR3 and CD56 were closely positioned to TRM in the Diffusion Map (Cluster 5 for CD4 and cluster 13 for CD8), suggesting that TRM may be derived from circulating CXCR3+ precursors.

Overall, this unbiased analysis is consistent with the view that the thyroid gland and the peripheral blood contain largely different types of T-cells. In particular, the thyroid CD8 compartment was enriched for TRM and effector-like cells, while actively proliferating CD8+T-cells and putative precursors of TRM were predominantly found in the blood.

3.6. Some T-cells in the thyroid gland display a tissue-resident phenotype

We then analyzed the T-cell compartments in the blood and the thyroid more in detail by conventional manual gating. The percentages of total CD4+ and CD8+ T-cells within thyroid were in general not different from those in peripheral blood (Fig. S6A). As shown in Fig. 6A, CD4+T-cells from the thyroid gland had however a more activated phenotype (CD38+ or CD69+) in COV-A-SAT and in particular in VAX-SAT patients. This was true not only as compared to paired blood samples, but also as compared to the thyroid of the autoimmune (ATD) cohort. In the CD8 compartment, we also detected a significantly increased CD69 expression in the thyroid glands in COV-A-SAT and VAX-SAT patients (Fig. 6A). Conversely, IL-7R$_{low}$ effector-like cells were more prominent in the thyroid of ATD and VAX-SAT patients.

Canonical CD103+CD69+ TRM were identified in both CD4+ and CD8+ T-cell subsets and, as expected, exclusively in the thyroid gland (Fig. 6B). Interestingly, with the caveat that we could analyze only a limited number of ATD patients, CD4+ TRM were restricted to COV-A-SAT and VAX-SAT patients (Fig. 6B). A phenotypic analysis of TRM in the thyroid unveiled that they expressed overall high levels of CD38 and CXCR3, but CD8+TRM had down-regulated CD27 (Fig. S6B). Interestingly, CD8+TRM in COV-A-SAT and VAX-SAT differed in IL-7R expression. Since intra-thyroid TRM were detectable only in a fraction of COV-A-SAT patients, we analyzed if their presence may depend on the analyzed time point. Although the mean frequencies of TRM were similar at the analyzed two time points, we noticed that, after eight months all analyzed COV-A-SAT patients contained TRM at least in the CD8 compartment, compared with only 3/8 (37%) after four months (Fig. 6C).

Overall, this analysis confirmed that CD4+ and CD8+ TRM-cells are present in the thyroid gland, and unveiled that TRM were consistently present at the later time point in COV-A-SAT patients.

3.7. SARS-CoV-2 specific TRM are present in the thyroid gland of COV-A-SAT patients after 8 months

To detect SARS-CoV-2-specific T-cells also in the thyroid, we first performed HLA haplotyping of all 13 COV-A-SAT patients (Table 1/2) to be able to identify such cells with suited SARS-CoV-2 peptide-HLA multimers (Table 3). Interestingly, we observed that HLA-DRB1*13 was significantly over-represented in the total cohort of 13 COV-A-SAT patients as compared to healthy haplotyped donors ($p=0.01$), suggesting that it may represent a genetic risk factor to develop COV-A-SAT. Moreover, there was also a significantly more frequent expression of HLA-B*57, suggesting that both CD4+ and CD8+ T-cell responses may

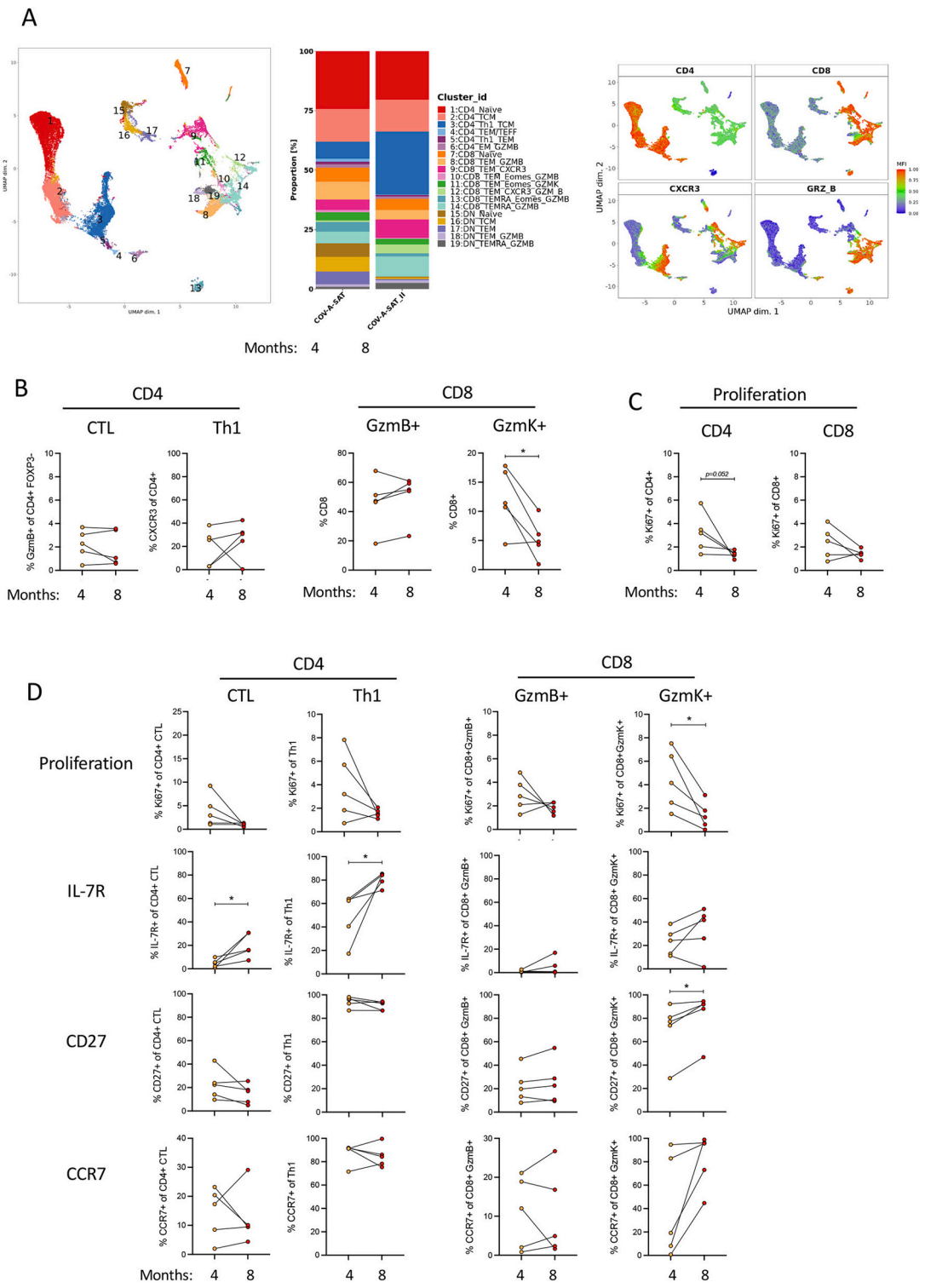

Fig. 3. Increased T-cell proliferation and effector cell generation in COV-A-SAT patients is transient.
COV-A-SAT patients (w/o ATD, $n = 5$) were analyzed after 4 and 8 months post-infection by multi-parametric flow cytometry.
A. Left: UMAP maps of the 19 identified T-cell clusters marked with different colors. Middle: Bar-plots showing selective cluster distributions after 4 and 8 months post-infection. Right: Two dimensionality illustration of CD4, CD8, CXCR3 and GZM_B expression level by UMAP. Red indicates high, green intermediate and blue low expression levels.
B: Percentages of CTL and Th1-cells among CD4+T-cells and of cytotoxic GzmB+GzmK- and GzmK+GzmB- cells among CD8 + T-cells.
C. Ex vivo expression of Ki67 in total CD4+ and CD8+ T-cells.
D. Ex vivo analysis of Ki67, IL-7R CD27 and CCR7 expression in CD4+CTL, Th1-cells, CD8+GzmB+ and CD8+ GzmK+ T-cells.
B-D: Lines connect the values of the same patients. Statistical analysis was performed with a paired student's *t*-test; < 0.05(*) were regarded as statistically significant.

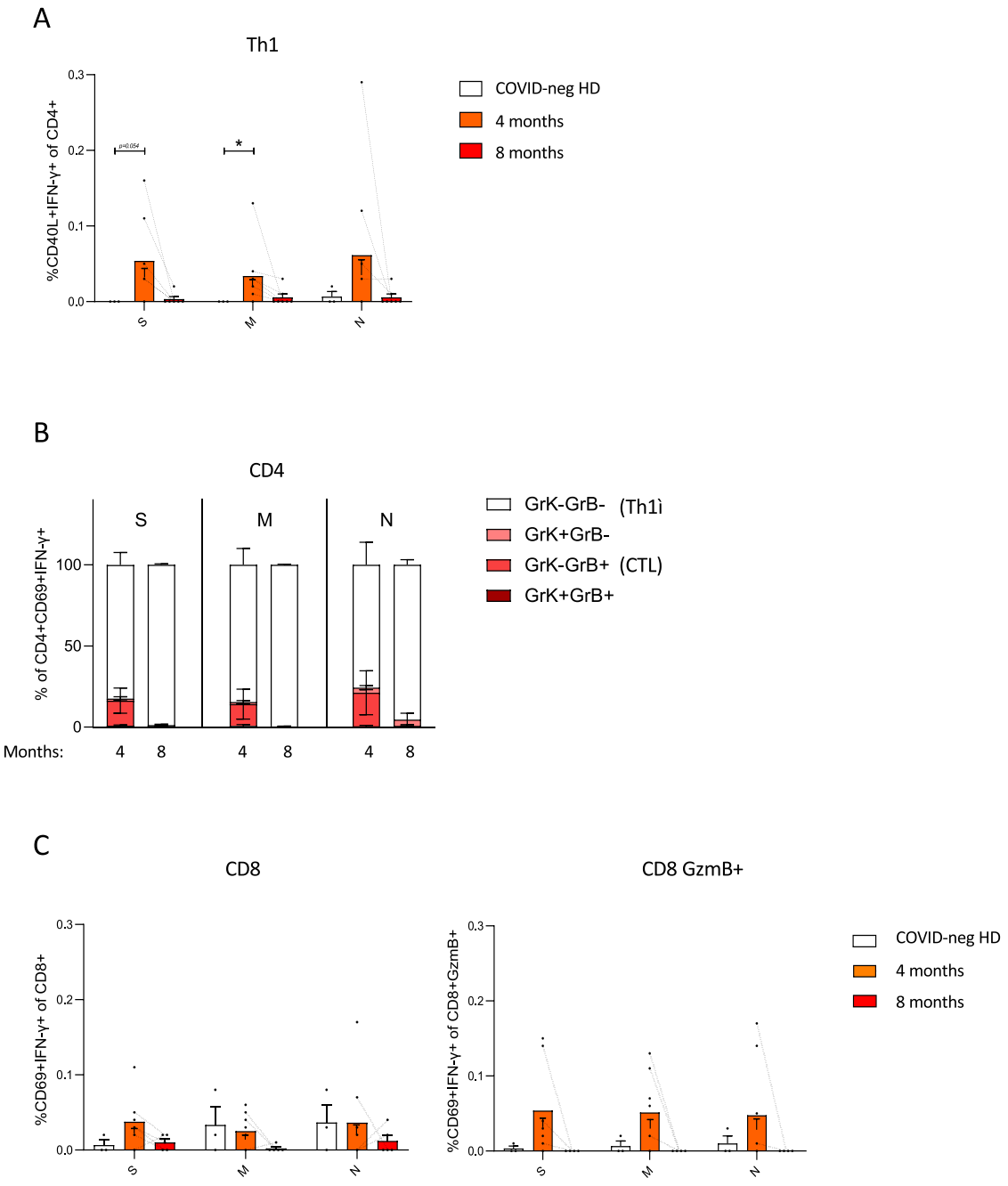

Fig. 4. SARS-CoV-2 specific T-cell responses in peripheral blood of COV-A-SAT patients are not sustained.

A. Frequencies of SARS-CoV-2 specific Th1-cells (CD4+CD40L+IFN-γ+) in the blood induced by peptide stimulation with COVID-19 peptides in COVID-naïve HDs ($n = 3$) and in COV-A-SAT patients 4 months and 8 months ($n = 7$) post-infection. Data show individual values, and the mean (bar height) ± SEM,

B. Percentages of COVID peptide-induced CD4+CD69+IFN-γ+ T-cells expressing GzmB and/or GzmK after stimulation with COVID-19 peptides at 4 months ($n = 6$) and 8 months post-infection ($n = 3$).

C. Frequencies of SARS-CoV-2 specific (CD69 + IFN-γ+) total CD8+ (left panel) or GzmB+ CD8+ (right panel) T-cells in COVID-naïve HDs ($n = 3$) and in COV-A-SAT patients 4 months ($n = 7$) and 8 months ($n = 5$) post-infection.

A, C: Values from the same patients at different time point are connected with a dotted line. Statistical analysis by Kruskal Wallis test; $p < 0.05$(*) were regarded as statistically significant.

contribute to the risk to develop COV-A-SAT. In any case, following HLA haplotyping, we were able to detect SARS-CoV-2-specific T-cells in peripheral blood and in the thyroid gland of eight COV-A-SAT patients (Fig. 7). SARS-COV-2-specific CD4+ and CD8+ T-cells were increased in the thyroid gland (in mean 2.46±1.75%) as compared to the blood (in mean 0.17±0.13%) as expected; for CD8+T-cells this difference reached statistical significance (Fig. 7A). When analyzing thyroid-derived T-cells for the expression of tissue-residency markers, a relevant fraction of SARS-CoV-2-specific T-cells were found to express CD103 and CD69, alone or in combination, in particular in the CD8 compartment (Fig. 7B). We then compared SARS-CoV-2-specific CD8+T-cells in patients that had undergone US-FNA after four or after eight months post-infection. At both time points, SARS-CoV-2-specific CTL could be detected at variable frequencies (Fig. 7C). Intriguingly, when the phenotypes of these SARS-CoV-2-specific CTL were analyzed, we observed that CD103 expression was low after 4 months, but was expressed on virtually all

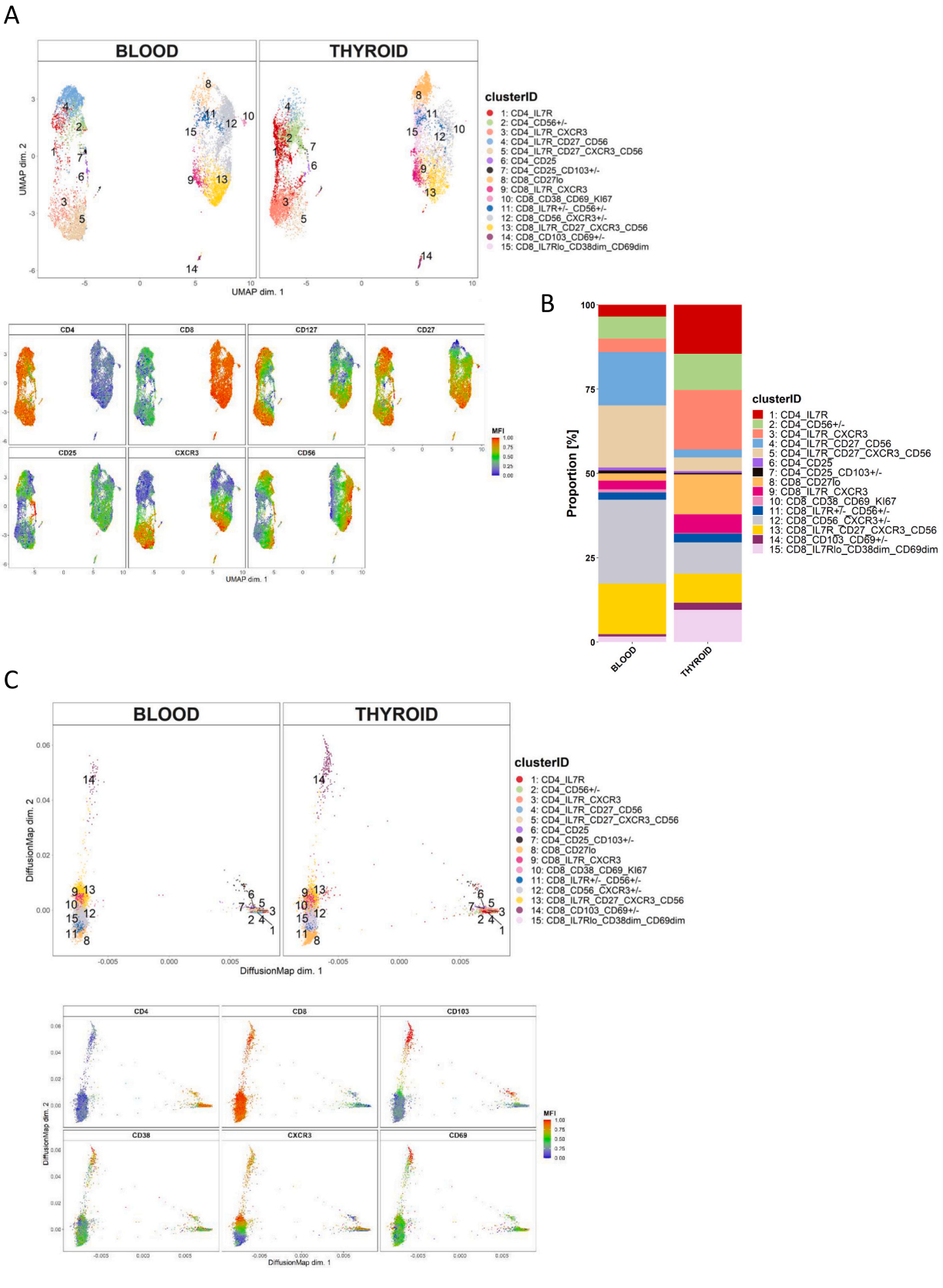

(caption on next page)

Fig. 5. The thyroid gland contains unique T-cell clusters.
A. UMAP maps of three different patients were colored according to 15 different CD4+ (left superclusters) and CD8+ T-cell clusters (right superclusters) in the blood and in the thyroid. Color code and phenotype of the 15 clusters is indicated in the Fig.
B. Two-dimensional illustration of CD4, CD8, CD127, CD27, CD25, CXCR3, CD56 and Ki67 expression in the UMAP maps. Blue denotes low, green intermediate and red high expression.
C. Bar-plots showing selective cluster distributions in the blood and the thyroid.
D. Possible cell differentiation was inferred by Diffusion Map and colored according to the identified T-cell clusters identified in A. Color code and phenotype of the 15 clusters is indicated. The CD103+ clusters (7, 14 and 15) are separated from CD103- clusters (1–6, 8–13).
E. CD4, CD8, CD103, CD38, CXCR3 and CD69 expression in the Diffusion Maps. Dimension 1 separates two superclusters of CD8+ (left) and CD4+ T-cells (right). Dimension 2 separates CD103+ (upper) from CD103- clusters (lower). Blue denotes low, green intermediate and red high expression.

cells after 8 months. Consequently, SARS-CoV-2-specific CD8 +T-cells with a canonical CD69+CD103+TRM phenotype were rare at the early time point, but abundant at the later time point (Fig. 7D).

Finally, we assessed possible cross-reactivities of SARS-COV2-specific T-cells and thyroid autoantigens (65). However, the homologies between the SARS-COV2-derived epitopes that we had assessed here (suplementary Table 2), and peptides derived from thyroid autoantigens (TPO, TSHR, TG) was overall low (max. 50%, suplementary Table 4). Moreover, most of these autoantigen-derived peptides were not predicted to be presented by the relevant MHC-I molecules (suplementary Table 4), suggesting that they are ignored by T-cells. A prediction of MHC class II epitopes with NetMHCIIpan 4.0 server failed to classify the two assessed epitopes (suplementary Table 2) as "strong binders" of HLA-DRB*07:01 (data not shown), and a reliable prediction of cross-reactive $CD4^{+}$T-cell epitopes was therefore not feasible. We also analyzed possible cross-reactivities of all epitopes derived from thyroid autoantigens that were predicted to be presented on the COV-A-SAT-associated MHC class I allele HLA-B*57:01 (suplementary Table 3). However, also in this case, the homologies with predicted epitopes derived from the Spike protein of SARS-COV2 was rather low (Range 18–56%, suplementary Table 5). Overall, this in silico analysis suggests that cross-reactivities of T-cells with thyroid autoantigens of the here analyzed epitopes and the COV-A-SAT-associated MHC class I haplotype is unlikely to play a major role.

In conclusion, our findings demonstrate that SARS-CoV-2 specific CD4+ and CD8+T-cells are present in the thyroid glands of COV-A-SAT patients. Moreover, SARS-CoV-2 specific T-cells in the thyroid acquired the phenotype of CD103+TRM cells at late time points.

4. Discussion

SARS-COV2 can infect a wide range of tissues since ACE2, the main entry receptor for SARS-CoV-2 [42,43], is broadly expressed, including thyroid cells [44,45]. We previously reported on atypical thyroiditis in patients hospitalized for moderate-to-severe Covid-19 [15,16] and here we analyzed their T-cell compartments in peripheral blood and the thyroid gland, with a focus on virus-specific CD4+ and CD8+ T-cells. The main strength of this study is the availability of precious samples (paired blood and thyroid-derived cells) collected in a cohort of patients with thyroid abnormalities related to moderate-to-severe Covid-19. Their immunological signature is unbiased, since studied before the administration of Covid-19 vaccines and thus only reflecting the effects of natural infection with SARS-CoV-2. These unique characteristics of the samples explain the relatively low number of Covid-19 patients with related thyroid dysfunction, and the impossibility to further increase the number of patients due to the subsequent start of the mass vaccination campaign. We compared these patients developing atypical subacute thyroiditis during moderate-to-severe Covid-19 disease (COV-A-SAT) [15,16] to patients with different thyroid disorders, such as classic SAT developed after Covid-19 vaccination and thyroid autoimmunity. Classic SAT is a transient non-autoimmune disorder usually triggered by viral infections [27,46], that has also been described following both SARS-CoV-2 infection [11,14] or Covid-19 vaccination [17–20]. In the long term permanent hypothyroidism may occur in 25% of SAT cases [47,48], while atypical thyroiditis associated with Covid-19 disease is characterized by a complete recovery of thyroid function [15,16]. Thyroid autoimmunity is the most frequent autoimmune disorder, with thyroid autoantibodies being positive in about 12% of general population [29,49]. Cases of Graves' disease and Graves' orbitopathy have also been described following both SARS-CoV-2 infection [50–53] and Covid-19 vaccination [21–26]. Besides environmental triggers, a genetic predisposition has a key role in the development of thyroid diseases [49,54,55]. Indeed, the majority of ATD and VAX-SAT patients had a positive family history for thyroid disorders, compared with only one COV-A-SAT patient. The HLA haplotype analysis of COV-A-SAT patients, which needs of course to be verified and confirmed in larger study cohorts, suggested a key role for T-cell responses. Thus, the allele HLA-DRB1*13 was present significantly more frequent among the here analyzed COV-A-SAT patients than in a cohort of >2000 HLA haplotyped donors of our hospital. Also the allele HLA-B*57 was present significantly more frequently than expected, suggesting that both CD4+ and CD8+T-cells contribute to the risk to develop COV-A-SAT. Conversely, alleles associated with classical SAT, such as HLA-Bw35, HLAB67, HLA-B15/62 or HLA-Drw8 [11,54] were not expressed more frequently among COV-A-SAT patients. Notably, ATD is not strongly associated with any specific HLA haplotype [56].

The main immunological finding of this study is that, despite a transient SARS-CoV-2-specific Th1- and cytotoxic effector T-cell response in peripheral blood, SARS-CoV-2-specific CD4+ and CD8+ T-cells persisted in the thyroid gland and acquired a canonical tissue-resident memory (TRM) phenotype, in particular at late time points. The transient nature of the systemic SARS-CoV-2-specific T-cell response was unexpected, since previous studies on circulating T-cells in conventional Covid-19 patients without reported thyroid involvement concluded that SARS-CoV-2-specific T-cell responses are sustained [4–6]. In particular, Covid-19-vaccination-induced CD8+T-cells in the blood that are specific for two S-derived epitopes presented on HLA*A24:02 were shown to be maintained long-term [6]. Notably, however, these epitope-specific CD8+T-cells cross-reacted with seasonal coronaviruses [6], and it is therefore unclear if the long-term persistence of these CD8 + T-cells is truly antigen-independent. In any case, we identified here CD8+T-cells specific for the same epitopes also in the thyroid of several HLA*A24:02+ patients eight months post-infection, in spite of the fact that total S-specific CD4+ and CD8+ T-cell responses in the blood were hardly detectable at this late time point. It is possible that the here analyzed patients have a unique behavior, and that SARS-CoV-2-specific T-cells disappear from the blood because they were retained in the thyroid and potentially also in other tissues. The reduction of systemic effector T-cells observed 8 months following infection is in line with the transient and self-limiting nature of Covid-19 related atypical thyroiditis [16].

The analysis of T-cells in the thyroid suggested that SARS-CoV-2-specific T-cells persist in this peculiar target organ, and acquire the phenotype of TRM cells, which are largely unable to recirculate through the blood. Overall, very little is known on the thyroid T-cell compartment, in particular in viral infections [9,10,46]. Our unbiased comparison of T-cells from the thyroid and the blood suggested that CD69+CD103+ TRM were selectively present in the thyroid, and were largely distinct from all other T-cells. Interestingly, Diffusion Map analysis, which predicts possible differentiation pathways in pseudo-

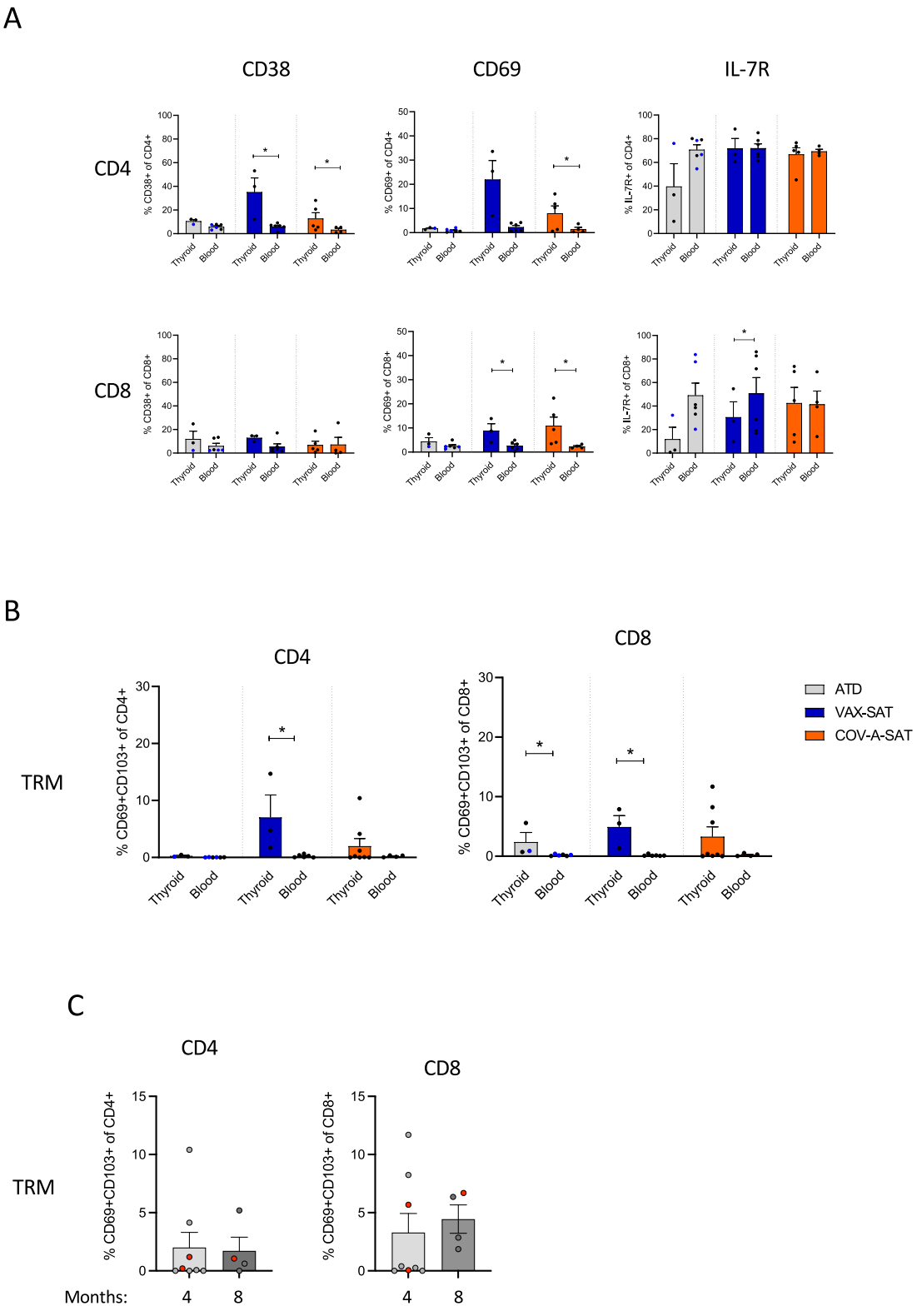

Fig. 6. Tissue-resident memory cells (TRM) are present in the thyroid gland.

A. Expression of CD38, CD69 and of IL-7R on CD4+ (upper panels) and CD8+ T-cells (lower panels) from thyroid US-FNA and peripheral blood of ATD patients (grey bars; blue dots: vaccinated, black dots not vaccinated patients; blood $n = 6$, thyroid $n = 3$), as well as of VAX-SAT (blue, blood $n = 6$, thyroid $n = 3$) and COV-A-SAT patients (non ATD, orange, blood $n = 4$, thyroid $n = 5$). Data show individual values, mean (bar height) ± SEM. Statistical analysis by Mann Whitney test; $p < 0.05$ (*) were regarded as statistically significant.

B. Percentage of CD103+CD69+TRM among CD4+ and CD8+T-cells in thyroid US-FNA and peripheral blood of ATD patients (grey, thyroid: $n = 3$, blood: $n = 6$) VAX-SAT patients (blue, thyroid $n = 3$, blood $n = 6$) and COV-A-SAT patients (orange, thyroid $n = 7$, blood $n = 4$).

C. Percentage of CD4+ and CD8+ TRM in the thyroids of COV-A-SAT patients 3 months ($n = 8$) and 8 months ($n = 4$) after COVID-19 infection. 2 Patients with concomitant ATD were included (marked in red).

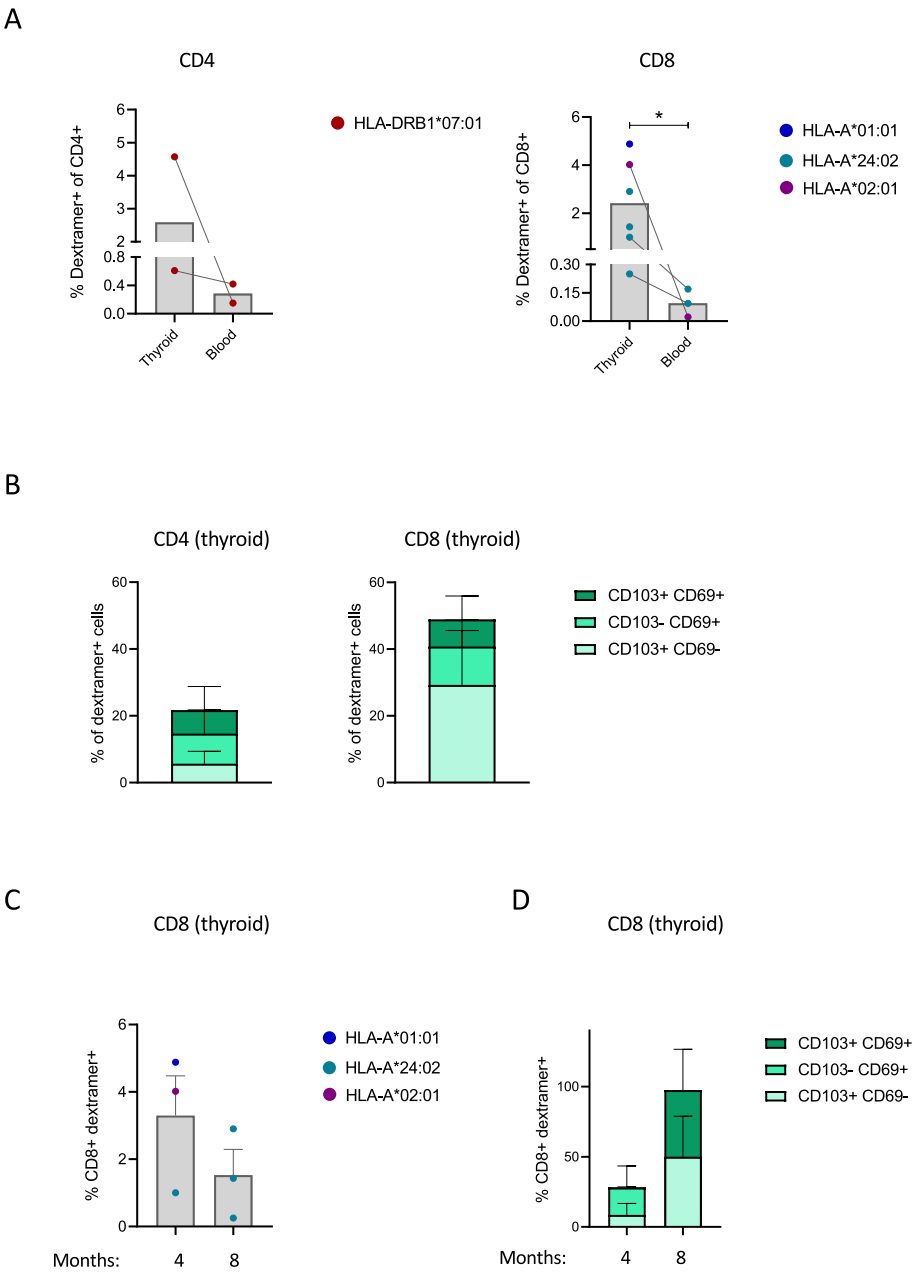

Fig. 7. SARS-CoV-2 specific T-cells in the thyroid acquire a TRM phenotype.

A. COVID-19-specific T-cells were identified in HLA haplotyped COV-A-SAT patients with appropriate peptide-MHC multimers (Table 2). COVID-19-specific CD4 + T-cells were detected in paired thyroid and blood samples of 2 HLA-DRB1*07:01 patients (left), one with and one w/o ATD. COVID-19-specific CD8+ T-cells (right) were detected in paired thyroid and blood samples (connected by lines) of 3 patients (1 HLA-A*02:01 (with ATD) and 2 HLA-A*24:02 (w/o ATD) and in 3 additional thyroid samples (all w/o ATD, 1 HLA-A*01:01 and 2 HLA-A*24:02). Data represent the frequencies of COVID-specific T-cells; the mean is indicated by grey bars. Statistical analysis was performed with a Mann Whitney test; $p < 0.05$(*) were regarded as statistically significant.

B. COVID-19-specific CD4+ ($n = 2$) and CD8+T-cells ($n = 6$) from thyroids were analyzed for CD69 and CD103 expression. The graphs report the percentages of cells expressing CD103 and CD69 alone or in combination. CD69+ CD103+TRM are shown in dark green, cells expressing CD69 or CD103 alone in light green as indicated. Data represent the mean percentages of CD69+ and/or CD103+ cells(error bars indicate SEM).

C. Percentages of COVID-19 epitope-specific CD8 + T-cells in thyroids at 3 ($n = 3$) and 8 months ($n = 3$) post-infection.

D. The same COVID-19-specific CD8+T-cells in thyroids were analyzed for CD69 and CD103 co-expression at 3 and 8 months post-infection. CD69+CD103+TRM are shown in dark green, cells expressing CD69 or CD103 alone in light green as indicated.

time dimension, suggested that TRM could be derived from CXCR3+T-cells, which were more abundant in the circulation. Thus, a possible scenario that is consistent with our data is an early recruitment of CXCR3+ TRM precursors from the blood to the thyroid, followed by a progressive local differentiation to TRM. Notably, CXCR3+CD4+ T-cells in the blood have anti-viral antigen specificities, and produce high levels of the anti-viral effector cytokine IFN-γ [34]. Consistently, our results indicate that TRM contained SARS-CoV-2-specific T-cells. Interestingly, some CD8+CXCR3+ T-cells in the blood expressed GzmK, a marker of putative memory precursor cells [5] that may switch to GzmB expression upon terminal CTL differentiation [39]. Consistent with the notion that they contained memory precursors, GzmK+CD8+ T-cells proliferated and displayed an effector phenotype in the early memory phase, but were reduced at later time points. Moreover, they acquired a memory phenotype and became largely resting.

TRM in Covid-19 patients have been identified previously in the lung [8], in the nose and the mucosa of the upper respiratory tract [57]. Importantly, TRM are in general long-lived, but TRM in the lung are apparently a Covid-19-relevant exception to this rule [8]. The presence of TRM in the thyroid gland was recently suggested by single-cell RNA sequencing in thyroid tumors [58], but this is to our best knowledge the first report that identifies TRM in the non-transformed thyroid gland. With the caveat that we could not analyze the thyroid of the same patients both at the early and the late time point, the late and dramatic increase of CD103 expression on COVID-specific CD8+T-cells suggests that COVID-specific TRM are generated with delayed kinetics as compared to the early and transient systemic effector T-cell response. As mentioned previously, since the virus was undetectable since several weeks in the blood and also in the thyroid target organ, we analyzed an early and late time point of memory generation in these patients. In Covid-19 related atypical thyroiditis the thyroid dysfunction is usually observed at early time points and is transient [15,16]. Therefore, the late generation of TRM might suggest a protective role against reinfections, rather than a detrimental pro-inflammatory role. However, signs of

inflammation at thyroid ultrasound persist up to one year post infection, thus an ongoing subclinical thyroid damage cannot be fully excluded in these patients [16]. TRM cells were also present in patients with no previous history of SARS-CoV-2 infection and thyroid disorders, who developed classic SAT shortly following Covid-19 vaccination. SARS-CoV-2 specificity and long-term maintenance of these vaccination-associated TRM could unfortunately not be analyzed [59], but it is possible that they contributed to thyroid tissue damage [60]. Indeed, dysfunctions of CD8+T-cells from bronchoalveolar lavage have been previously associated with post Covid-19 disease lung sequelae, but the canonical CD103+TRM analyzed in that study in the thyroid had only a low pathogenic potential [61]. Indeed, Covid-19-induced organ damaging could also be explained by several other mechanisms [62]. First, the SARS-CoV-2 spike has an intrinsic toxic activity [63] and circulates through blood to several organs [64] including the thyroid [44,45]. Second, an immunological cross-reactivity could be triggered, by revelation of cryptic antigens or molecular mimicry of the spike protein or other viral components with self-antigens [65]. Indeed, Vojdani et al. have identified a 50–70% sequence homology between TPO and SARS-CoV-2-derived proteins or peptides, especially the spike. They also demonstrated a cross-reactivity of anti-SARS-CoV-2 spike, nucleocapsid and membrane antibodies with TPO protein (65). Our in silico analysis did not unveil major cross-reactivities between SARS-CoV-2 MHC class I epitopes used in this study and the main thyroid autoantigens. A possible molecular mimicry of thyroid autoantigen- and SARS-CoV2-derived epitopes presented on the COV-A-SAT risk allele HLA-B*57:01 was also rather unlikely. We can however of course not rule out that other SARS-COV2-derived epitopes, in particular those presented on MHC class II, may be cross-reactive with thyroid self-peptides. However, since only 15% of COV-A-SAT patients contained anti-thyroid autoantibodies (Table 1), a percentage in line with the prevalence in the general population, this seems rather unlikely, since cross-reactive CD4+ T-cells may provide help not only for anti-SARS-COV2-specific antibodies, but also promote autoantibody production.

In conclusion, we showed that Covid-19 associated non-autoimmune thyroiditis, is characterized by the generation of SARS-COV-2-specific, tissue-resident memory T-cells in the thyroid, which were present after several months post-infection. This finding has relevant implications for the maintenance of SARS-COV2-specific T-cell memory in tissues, and shows that tissue-resident memory cells can contribute to antiviral immune responses in the thyroid. Further studies, including mouse models, are needed to explore their potential role in the pathogenesis of thyroid damage, and to verify whether they are also present in Covid-19 patients who did not develop thyroid abnormalities.

Fundings

This study was funded by the European Society of Endocrinology (ESE) Covid-19 Research Grant to Ilaria Muller. It was also partially supported by Ricerca Corrente Funds from the Italian Ministry of Health to Fondazione IRCCS Ca' Granda Ospedale Maggiore Policlinico Milan. Jens Geginat is supported by AIRC, IG 23581.

Declaration of Competing Interest

We declare no conflict of interest.

Data availability

No data was used for the research described in the article.

Acknowledgments

We thank the patients involved in this study and Dr. Giovanna Lunghi e Prof Ferruccio Ceriotti (UOC Laboratorio Analisi Fondazione IRCCS Ca' Granda Ospedale Maggiore Policlinico di Milano) for providing the analysis of intra-thyroid SARS-CoV-2 RNA. We thank Samuele Nortabartolo for critical reading and Discussion of the manuscript.

Appendix A. Supplementary data

Supplementary data to this article can be found online at https://doi.org/10.1016/j.clim.2023.109684.

References

[1] E. Dong, H. Du, L. Gardner, An interactive web-based dashboard to track COVID-19 in real time, Lancet Infect. Dis. 20 (2020) 30120–30121.
[2] L. Dai, G.F. Gao, Viral targets for vaccines against COVID-19, Nat. Rev. Immunol. 21 (2021) 73–82.
[3] F. Kreier, Ten billion COVID vaccinations: world hits new milestone, Nature 31 (2022).
[4] L.B. Rodda, J. Netland, L. Shehata, K.B. Pruner, P.A. Morawski, C.D. Thouvenel, K. K. Takehara, J. Eggenberger, E.A. Hemann, H.R. Waterman, M.L. Fahning, Y. Chen, M. Hale, J. Rathe, C. Stokes, S. Wrenn, B. Fiala, L. Carter, J.A. Hamerman, N. P. King, M. Gale Jr., D.J. Campbell, D.J. Rawlings, M. Pepper, Functional SARS-CoV-2-specific immune memory persists after mild COVID-19, Cell 184 (2021) 169–183 (e117).
[5] S. Notarbartolo, V. Ranzani, A. Bandera, P. Gruarin, V. Bevilacqua, A.R. Putignano, A. Gobbini, E. Galeota, C. Manara, M. Bombaci, E. Pesce, E. Zagato, A. Favalli, M.L. Sarnicola, S. Curti, M. Crosti, M. Martinovic, T. Fabbris, F. Marini, L. Donnici, M. Lorenzo, M. Mancino, R. Ungaro, A. Lombardi, D. Mangioni, A. Muscatello, S. Aliberti, F. Blasi, T. De Feo, D. Prati, L. Manganaro, F. Granucci, A. Lanzavecchia, R. De Francesco, A. Gori, R. Grifantini, S. Abrignani, Integrated longitudinal immunophenotypic, transcriptional and repertoire analyses delineate immune responses in COVID-19 patients, Sci. Immunol. 6 (2021) eabg5021.
[6] N. Kuse, Y. Zhang, T. Chikata, H.T. Nguyen, S. Oka, H. Gatanaga, M. Takiguchi, Long-term memory CD8(+) T cells specific for SARS-CoV-2 in individuals who received the BNT162b2 mRNA vaccine, Nat. Commun. 13 (2022) 5251.
[7] D.L. Turner, K.L. Bickham, J.J. Thome, C.Y. Kim, F. D'Ovidio, E.J. Wherry, D. L. Farber, Lung niches for the generation and maintenance of tissue-resident memory T cells, Mucosal Immunol. 7 (2014) 501–510.
[8] F.R. Carbone, Unique properties of tissue-resident memory T cells in the lungs: implications for COVID-19 and other respiratory diseases, Nat. Rev. Immunol. (2022) 1–7.
[9] A. Geslot, P. Chanson, P. Caron, Covid-19, the thyroid and the pituitary - the real state of play, Ann. Endocrinol. (Paris) 83 (2022) 103–108.
[10] M. Darvishi, M.R. Nazer, H. Shahali, M. Nouri, Association of thyroid dysfunction and COVID-19: a systematic review and meta-analysis, Front. Endocrinol. (Lausann.) 13 (2022), 947594.
[11] A. Brancatella, D. Ricci, N. Viola, D. Sgro, F. Santini, F. Latrofa, Subacute thyroiditis after Sars-COV-2 infection, J. Clin. Endocrinol. Metab. 105 (2020).
[12] A. Lania, M.T. Sandri, M. Cellini, M. Mirani, E. Lavezzi, G. Mazziotti, Thyrotoxicosis in patients with COVID-19: the THYRCOV study, Eur. J. Endocrinol. 183 (2020) 381–387.
[13] W. Chen, Y. Tian, Z. Li, J. Zhu, T. Wei, J. Lei, Potential interaction between SARS-CoV-2 and thyroid: a review, Endocrinology 162 (2021).
[14] J. Christensen, K. O'Callaghan, H. Sinclair, K. Hawke, A. Love, K. Hajkowicz, A. G. Stewart, Risk factors, treatment and outcomes of subacute thyroiditis secondary to COVID-19: a systematic review, Intern. Med. J. 52 (2022) 522–529.
[15] I. Muller, D. Cannavaro, D. Dazzi, D. Covelli, G. Mantovani, A. Muscatello, E. Ferrante, E. Orsi, V. Resi, V. Longari, M. Cuzzocrea, A. Bandera, E. Lazzaroni, A. Dolci, F. Ceriotti, T.E. Re, A. Gori, M. Arosio, M. Salvi, SARS-CoV-2-related atypical thyroiditis, Lancet Diabetes Endocrinol. 8 (2020) 739–741.
[16] I. Muller, A. Daturi, M. Varallo, T.E. Re, D. Dazzi, S. Maioli, E. Crivicich, F. Di Marco, V. Longari, B. Dazzi, M. Castellani, G. Mantovani, M. Arosio, M. Salvi, Long-term outcome of thyroid abnormalities in patients with severe Covid-19, Eur. Thyroid. J. 12 (2023), e220200.
[17] K.A. Lee, Y.J. Kim, H.Y. Jin, Thyrotoxicosis after COVID-19 vaccination: seven case reports and a literature review, Endocrine 74 (2021) 470–472.
[18] M. Pandya, G. Thota, X. Wang, H. Luo, Thyroiditis after Coronavirus Disease 2019 (COVID-19) mRNA Vaccine: A Case Series, AACE Clin Case Rep 8 (2021) 118.
[19] L. Das, S.K. Bhadada, A. Sood, Post-COVID-vaccine autoimmune/inflammatory syndrome in response to adjuvants (ASIA syndrome) manifesting as subacute thyroiditis, J. Endocrinol. Investig. 45 (2022) 465–467.
[20] W.M. Bennet, A. Elamin, J.D. Newell-Price, Subacute thyroiditis following COVID-19 vaccination: case report and Society for Endocrinology survey, Clin. Endocrinol. (Oxf). 98 (2023) 452–453.
[21] A. Pujol, L.A. Gomez, C. Gallegos, J. Nicolau, P. Sanchis, M. Gonzalez-Freire, A. A. Lopez-Gonzalez, K. Dotres, L. Masmiquel, Thyroid as a target of adjuvant autoimmunity/inflammatory syndrome due to mRNA-based SARS-CoV2 vaccination: from Graves' disease to silent thyroiditis, J. Endocrinol. Investig. 45 (2022) 875–882.
[22] M.A. Weintraub, B. Ameer, N. Sinha Gregory, Graves disease following the SARS-CoV-2 vaccine: case series, J. Investig. Med. High Impact Case Rep. 9 (2021), 23247096211063356.
[23] G. Zettinig, M. Krebs, Two further cases of Graves' disease following SARS-Cov-2 vaccination, J. Endocrinol. Investig. 45 (2022) 227–228.

[24] D. Kikkawa, K. Park, S. Fung, M. Ting, D. Ozzello, J. Yoon, C. Liu, B. Korn, Thyroid eye disease reactivation associated with COVID-19 vaccination, Taiwan J. Ophthalmol. 12 (2022) 93–96.
[25] R. Manta, C. Martin, V. Muls, K.G. Poppe, New-onset Graves' disease following SARS-CoV-2 vaccination: a case report, Eur. Thyroid. J. 11 (2022), e220049.
[26] L. di Filippo, L. Castellino, A. Allora, S. Frara, R. Lanzi, F. Perticone, F. Valsecchi, A. Vassallo, R. Giubbini, C.J. Rosen, A. Giustina, Distinct clinical features of post COVID-19 vaccination early-onset Graves' disease (PoVEO GD), J. Clin. Endocrinol. Metab. 108 (2022) 107–113.
[27] E. Nishihara, H. Ohye, N. Amino, K. Takata, T. Arishima, T. Kudo, M. Ito, S. Kubota, S. Fukata, A. Miyauchi, Clinical characteristics of 852 patients with subacute thyroiditis before treatment, Intern. Med. 47 (2008) 725–729.
[28] L. Bartalena, G.J. Kahaly, L. Baldeschi, C.M. Dayan, A. Eckstein, C. Marcocci, M. Marino, B. Vaidya, W.M. Wiersinga, E. Dagger, The 2021 European group on Graves' orbitopathy (EUGOGO) clinical practice guidelines for the medical management of Graves' orbitopathy, Eur. J. Endocrinol. 185 (2021) G43–G67.
[29] M.P. Vanderpump, The epidemiology of thyroid disease, Br. Med. Bull. 99 (2011) 39–51.
[30] A. Cossarizza, H.D. Chang, A. Radbruch, S. Abrignani, R. Addo, M. Akdis, I. Andra, F. Andreata, F. Annunziato, E. Arranz, P. Bacher, S. Bari, V. Barnaba, J. Barros-Martins, D. Baumjohann, C.G. Beccaria, D. Bernardo, D.A. Boardman, J. Borger, C. Bottcher, L. Brockmann, M. Burns, D.H. Busch, G. Cameron, I. Cammarata, A. Cassotta, Y. Chang, F.G. Chirdo, E. Christakou, L. Cicin-Sain, L. Cook, A. J. Corbett, R. Cornelis, L. Cosmi, M.S. Davey, S. De Biasi, G. De Simone, G. Del Zotto, M. Delacher, F. Di Rosa, J. Di Santo, A. Diefenbach, J. Dong, T. Dorner, R. J. Dress, C.A. Dutertre, S.B.G. Eckle, P. Eede, M. Evrard, C.S. Falk, M. Feuerer, S. Fillatreau, A. Fiz-Lopez, M. Follo, G.A. Foulds, J. Frobel, N. Gagliani, G. Galletti, A. Gangaev, N. Garbi, J.A. Garrote, J. Geginat, N.A. Gherardin, L. Gibellini, F. Ginhoux, D.I. Godfrey, P. Gruarin, C. Haftmann, L. Hansmann, C.M. Harpur, A. C. Hayday, G. Heine, D.C. Hernandez, M. Herrmann, O. Hoelsken, Q. Huang, S. Huber, J.E. Huber, J. Huehn, M. Hundemer, W.Y.K. Hwang, M. Iannacone, S. M. Ivison, H.M. Jack, P.K. Jani, B. Keller, N. Kessler, S. Ketelaars, L. Knop, J. Knopf, H.F. Koay, K. Kobow, K. Kriegsmann, H. Kristyanto, A. Krueger, J.F. Kuehne, H. Kunze-Schumacher, P. Kvistborg, I. Kwok, D. Latorre, D. Lenz, M.K. Levings, A. C. Lino, F. Liotta, H.M. Long, E. Lugli, K.N. MacDonald, L. Maggi, M.K. Maini, F. Mair, C. Manta, R.A. Manz, M.F. Mashreghi, A. Mazzoni, J. McCluskey, H.E. Mei, F. Melchers, S. Melzer, D. Mielenz, L. Monin, L. Moretta, G. Multhoff, L.E. Munoz, M. Munoz-Ruiz, F. Muscate, A. Natalini, K. Neumann, L.G. Ng, A. Niedobitek, J. Niemz, L.N. Almeida, S. Notarbartolo, L. Ostendorf, L.J. Pallett, A.A. Patel, G. I. Percin, G. Peruzzi, M. Pinti, A.G. Pockley, K. Pracht, I. Prinz, I. Pujol-Autonell, N. Pulvirenti, L. Quatrini, K.M. Quinn, H. Radbruch, H. Rhys, M.B. Rodrigo, C. Romagnani, C. Saggau, S. Sakaguchi, F. Sallusto, L. Sanderink, I. Sandrock, C. Schauer, A. Scheffold, H.U. Scherer, M. Schiemann, F.A. Schildberg, K. Schober, J. Schoen, W. Schuh, T. Schuler, A.R. Schulz, S. Schulz, J. Schulze, S. Simonetti, J. Singh, K.M. Sitnik, R. Stark, S. Starossom, C. Stehle, F. Szelinski, L. Tan, A. Tarnok, J. Tornack, T.I.M. Tree, J.J.P. van Beek, W. van de Veen, K. van Gisbergen, C. Vasco, N.A. Verheyden, A. von Borstel, K.A. Ward-Hartstonge, K. Warnatz, C. Waskow, A. Wiedemann, A. Wilharm, J. Wing, O. Wirz, J. Wittner, J.H.M. Yang, J. Yang, Guidelines for the use of flow cytometry and cell sorting in immunological studies (third edition), Eur. J. Immunol. 51 (2021) 2708–3145.
[31] M. Nowicka, C. Krieg, H.L. Crowell, L.M. Weber, F.J. Hartmann, S. Guglietta, B. Becher, M.P. Levesque, M.D. Robinson, CyTOF workflow: differential discovery in high-throughput high-dimensional cytometry datasets, F1000Res 6 (2017) 748.
[32] B. Reynisson, B. Alvarez, S. Paul, B. Peters, M. Nielsen, NetMHCpan-4.1 and NetMHCIIpan-4.0: improved predictions of MHC antigen presentation by concurrent motif deconvolution and integration of MS MHC eluted ligand data, Nucleic Acids Res. 48 (2020) W449–W454.
[33] F. Sallusto, J. Geginat, A. Lanzavecchia, Central memory and effector memory T cell subsets: function, generation, and maintenance, Annu. Rev. Immunol. 22 (2004) 745–763.
[34] L. Rivino, M. Messi, D. Jarrossay, A. Lanzavecchia, F. Sallusto, J. Geginat, Chemokine receptor expression identifies pre-T helper (Th)1, pre-Th2, and nonpolarized cells among human CD4+ central memory T cells, J. Exp. Med. 200 (2004) 725–735.
[35] J. Geginat, C. Vasco, P. Gruarin, R. Bonnal, G. Rossetti, Y. Silvestri, E. Carelli, N. Pulvirenti, M. Scantamburlo, G. Moschetti, F. Clemente, F. Grassi, S. Monticelli, M. Pagani, S. Abrignani, EOMESODERMIN-expressing type 1 regulatory (EOMES(+) Tr1)-like T-cells: basic biology and role in immune-mediated diseases, Eur. J. Immunol. 53 (2023), e2149775.
[36] D. Hamann, P.A. Baars, M.H. Rep, B. Hooibrink, S.R. Kerkhof-Garde, M.R. Klein, R. A. van Lier, Phenotypic and functional separation of memory and effector human CD8+ T cells, J. Exp. Med. 186 (1997) 1407–1418.
[37] L. Lozza, L. Rivino, G. Guarda, D. Jarrossay, A. Rinaldi, F. Bertoni, F. Sallusto, A. Lanzavecchia, J. Geginat, The strength of T cell stimulation determines IL-7 responsiveness, secondary expansion, and lineage commitment of primed human CD4+IL-7Rhi T cells, Eur. J. Immunol. 38 (2008) 30–39.
[38] B. Haringer, L. Lozza, B. Steckel, J. Geginat, Identification and characterization of IL-10/IFN-gamma-producing effector-like T cells with regulatory function in human blood, J. Exp. Med. 206 (2009) 1009–1017.
[39] K. Bratke, M. Kuepper, B. Bade, J.C. Virchow Jr., W. Luttmann, Differential expression of human granzymes a, B, and K in natural killer cells and during CD8+ T cell differentiation in peripheral blood, Eur. J. Immunol. 35 (2005) 2608–2616.
[40] C.J. Pitcher, S.I. Hagen, J.M. Walker, R. Lum, B.L. Mitchell, V.C. Maino, M. K. Axthelm, L.J. Picker, Development and homeostasis of T cell memory in rhesus macaque, J. Immunol. 168 (2002) 29–43.
[41] I. Kastirr, M. Crosti, S. Maglie, M. Paroni, B. Steckel, M. Moro, M. Pagani, S. Abrignani, J. Geginat, Signal strength and metabolic requirements control cytokine-induced Th17 differentiation of uncommitted human T cells, J. Immunol. 195 (2015) 3617–3627.
[42] R. Lu, X. Zhao, J. Li, P. Niu, B. Yang, H. Wu, W. Wang, H. Song, B. Huang, N. Zhu, Y. Bi, X. Ma, F. Zhan, L. Wang, T. Hu, H. Zhou, Z. Hu, W. Zhou, L. Zhao, J. Chen, Y. Meng, J. Wang, Y. Lin, J. Yuan, Z. Xie, J. Ma, W.J. Liu, D. Wang, W. Xu, E. C. Holmes, G.F. Gao, G. Wu, W. Chen, W. Shi, W. Tan, Genomic characterisation and epidemiology of 2019 Novel coronavirus: implications for virus origins and receptor binding, Lancet 395 (2020) 565–574.
[43] P. Zhou, X.L. Yang, X.G. Wang, B. Hu, L. Zhang, W. Zhang, H.R. Si, Y. Zhu, B. Li, C. L. Huang, H.D. Chen, J. Chen, Y. Luo, H. Guo, R.D. Jiang, M.Q. Liu, Y. Chen, X. R. Shen, X. Wang, X.S. Zheng, K. Zhao, Q.J. Chen, F. Deng, L.L. Liu, B. Yan, F. X. Zhan, Y.Y. Wang, G.F. Xiao, Z.L. Shi, A pneumonia outbreak associated with a new coronavirus of probable bat origin, Nature 579 (2020) 270–273.
[44] M.Y. Li, L. Li, Y. Zhang, X.S. Wang, Expression of the SARS-CoV-2 cell receptor gene ACE2 in a wide variety of human tissues, Infect. Dis. Povert. 9 (2020) 45.
[45] E. Lazartigues, M.M.F. Qadir, F. Mauvais-Jarvis, Endocrine significance of SARS-CoV-2's reliance on ACE2, Endocrinology 161 (2020).
[46] R. Desailloud, D. Hober, Viruses and thyroiditis: an update, Virol. J. 6 (2009) 5.
[47] V. Fatourechi, J.P. Aniszewski, G.Z. Fatourechi, E.J. Atkinson, S.J. Jacobsen, Clinical features and outcome of subacute thyroiditis in an incidence cohort: Olmsted County, Minnesota, study, J. Clin. Endocrinol. Metab. 88 (2003) 2100–2105.
[48] J. Gorges, J. Ulrich, C. Keck, D. Muller-Wieland, S. Diederich, O.E. Janssen, Long-term outcome of subacute thyroiditis, Exp. Clin. Endocrinol. Diabetes 128 (2020) 703–708.
[49] M.F. Prummel, T. Strieder, W.M. Wiersinga, The environment and autoimmune thyroid diseases, Eur. J. Endocrinol. 150 (2004) 605–618.
[50] M. Mateu-Salat, E. Urgell, A. Chico, SARS-COV-2 as a trigger for autoimmune disease: report of two cases of Graves' disease after COVID-19, J. Endocrinol. Investig. 43 (2020) 1527–1528.
[51] S. Jimenez-Blanco, B. Pla-Peris, M. Marazuela, COVID-19: a cause of recurrent Graves' hyperthyroidism? J. Endocrinol. Investig. 44 (2021) 387–388.
[52] A. Harris, M. Al Mushref, Graves' Thyrotoxicosis following SARS-CoV-2 infection, AACE Clin. Case Rep. 7 (2021) 14–16.
[53] G. Lanzolla, C. Marcocci, M. Marino, Graves' disease and Graves' orbitopathy following COVID-19, J. Endocrinol. Investig. 44 (2021) 2011–2012.
[54] N. Ohsako, H. Tamai, T. Sudo, T. Mukuta, H. Tanaka, K. Kuma, A. Kimura, T. Sasazuki, Clinical characteristics of subacute thyroiditis classified according to human leukocyte antigen typing, J. Clin. Endocrinol. Metab. 80 (1995) 3653–3656.
[55] B. Vaidya, P. Kendall-Taylor, S.H. Pearce, The genetics of autoimmune thyroid disease, J. Clin. Endocrinol. Metab. 87 (2002) 5385–5397.
[56] E.M. Jacobson, A. Huber, Y. Tomer, The HLA gene complex in thyroid autoimmunity: from epidemiology to etiology, J. Autoimmun. 30 (2008) 58–62.
[57] A.H.E. Roukens, C.R. Pothast, M. Konig, W. Huisman, T. Dalebout, T. Tak, S. Azimi, Y. Kruize, R.S. Hagedoorn, M. Zlei, F.J.T. Staal, F.J. de Bie, J.J.M. van Dongen, S. M. Arbous, J.L.H. Zhang, M. Verheij, C. Prins, A.M. van der Does, P.S. Hiemstra, J. J.C. de Vries, J.J. Janse, M. Roestenberg, S.K. Myeni, M. Kikkert, M. Yazdanbakhsh, M.H.M. Heemskerk, H.H. Smits, S.P. Jochems, B.-C.g. in collaboration with, C.-L.g. in collaboration with, prolonged activation of nasal immune cell populations and development of tissue-resident SARS-CoV-2-specific CD8(+) T cell responses following COVID-19, Nat. Immunol. 23 (2022) 23–32.
[58] T. Wang, J. Shi, L. Li, X. Zhou, H. Zhang, X. Zhang, Y. Wang, L. Liu, L. Sheng, Single-cell transcriptome analysis reveals inter-tumor heterogeneity in bilateral papillary thyroid carcinoma, Front. Immunol. 13 (2022), 840811.
[59] M. Hassert, J.T. Harty, Tissue resident memory T cells- a new benchmark for the induction of vaccine-induced mucosal immunity, Front. Immunol. 13 (2022) 1039194.
[60] N.P. Goplen, I.S. Cheon, J. Sun, Age-related dynamics of lung-resident memory CD8(+) T cells in the age of COVID-19, Front. Immunol. 12 (2021), 636118.
[61] I.S. Cheon, C. Li, Y.M. Son, N.P. Goplen, Y. Wu, T. Cassmann, Z. Wang, X. Wei, J. Tang, Y. Li, H. Marlow, S. Hughes, L. Hammel, T.M. Cox, E. Goddery, K. Ayasoufi, D. Weiskopf, J. Boonyaratanakornkit, H. Dong, H. Li, R. Chakraborty, A.J. Johnson, E. Edell, J.J. Taylor, M.H. Kaplan, A. Sette, B.J. Bartholmai, R. Kern, R. Vassallo, J. Sun, Immune signatures underlying post-acute COVID-19 lung sequelae, Sci. Immunol. 6 (2021) eabk1741.
[62] A. Dotan, S. Muller, D. Kanduc, P. David, G. Halpert, Y. Shoenfeld, The SARS-CoV-2 as an instrumental trigger of autoimmunity, Autoimmun. Rev. 20 (2021), 102792.
[63] Y. Lei, J. Zhang, C.R. Schiavon, M. He, L. Chen, H. Shen, Y. Zhang, Q. Yin, Y. Cho, L. Andrade, G.S. Shadel, M. Hepokoski, T. Lei, H. Wang, J. Zhang, J.X. Yuan, A. Malhotra, U. Manor, S. Wang, Z.Y. Yuan, J.Y. Shyy, SARS-CoV-2 spike protein impairs endothelial function via downregulation of ACE 2, Circ. Res. 128 (2021) 1323–1326.
[64] A.F. Ogata, C.A. Cheng, M. Desjardins, Y. Senussi, A.C. Sherman, M. Powell, L. Novack, S. Von, X. Li, L.R. Baden, D.R. Walt, Circulating severe acute respiratory syndrome coronavirus 2 (SARS-CoV-2) vaccine antigen detected in the plasma of mRNA-1273 vaccine recipients, Clin. Infect. Dis. 74 (2022) 715–718.
[65] A. Vojdani, E. Vojdani, D. Kharrazian, Reaction of human monoclonal antibodies to SARS-CoV-2 proteins with tissue antigens: implications for autoimmune diseases, Front. Immunol. 11 (2020), 617089.